

NPY₁R-targeted peptide-mediated delivery of a dual PPAR α/γ agonist to adipocytes enhances adipogenesis and prevents diabetes progression



Stefanie Wittrisch¹, Nora Klötting^{2,***}, Karin Mörl¹, Rima Chakaroun^{2,3}, Matthias Blüher^{2,3,***}, Annette G. Beck-Sickinger^{1,*}

ABSTRACT

Objective: PPAR α/γ dual agonists have been in clinical development for the treatment of metabolic diseases including type 2 diabetes and dyslipidemia. However, severe adverse side effects led to complications in clinical trials. As most of the beneficial effects rely on the compound activity in adipocytes, the selective targeting of this cell type is a cutting-edge strategy to develop safe anti-diabetic drugs. The goal of this study was to strengthen the adipocyte-specific uptake of the PPAR α/γ agonist tesaglitazar via NPY₁R-mediated internalization.

Methods: NPY₁R-preferring peptide tesaglitazar-[F⁷, P³⁴]-NPY (tesa-NPY) was synthesized by a combination of automated SPPS and manual couplings. Following molecular and functional analyses for proof of concept, cell culture experiments were conducted to monitor the effects on adipogenesis. Mice treated with peptide drug conjugates or vehicle either by gavage or intraperitoneal injection were characterized phenotypically and metabolically. Histological analysis and transcriptional profiling of the adipose tissue were performed.

Results: In vitro studies revealed that the tesaglitazar-[F⁷, P³⁴]-NPY conjugate selectively activates PPAR γ in NPY₁R-expressing cells and enhances adipocyte differentiation and adiponectin expression in adipocyte precursor cells. In vivo studies using *db/db* mice demonstrated that the anti-diabetic activity of the peptide conjugate is as efficient as that of systemically administered tesaglitazar. Additionally, tesa-NPY induces adipocyte differentiation in vivo.

Conclusions: The use of the tesaglitazar-[F⁷, P³⁴]-NPY conjugate is a promising strategy to apply the beneficial PPAR α/γ effects in adipocytes while potentially omitting adverse effects in other tissues.

© 2019 The Authors. Published by Elsevier GmbH. This is an open access article under the CC BY license (<http://creativecommons.org/licenses/by/4.0/>).

Keywords Adipocyte targeting; NPY₁R; Peptide drug conjugate; Tesaglitazar; Type 2 diabetes

1. INTRODUCTION

Obesity is a global epidemic that continues to rise and consequently results in the increased occurrence of associated metabolic disorders such as type 2 diabetes (T2D) and cardiovascular diseases [1–3]. An imbalance between energy expenditure and energy intake leads to an increased storage of lipids in adipose tissue. This excess fat can either be stored in newly differentiated adipocytes, resulting in an increased cell number (hyperplasia), or in already existing adipocytes, causing enlarged cells (hypertrophy) [4]. While hyperplastic adipocytes seem to be metabolically risk-free, hypertrophy has been linked to the

development of metabolic diseases [5,6]. The amount of adipocytes is mainly determined during childhood and adolescence, and as a result, hypertrophy is the preferred mechanism for the extension of adipose tissue as the ability of de novo adipogenesis is often exceeded in obese patients [4,7]. Peroxisome proliferator-activated receptor gamma (PPAR γ) agonists are known for their outstanding anti-diabetic potential as they promote adipogenesis and lead to the development of small, metabolically healthy adipocytes [8–12]. However, these molecules further regulate a variety of processes in other cell types [13,14]. Therefore, the clinical application of some PPAR γ agonists is accompanied by side effects including congestive heart failure,

¹Universität Leipzig, Institute of Biochemistry, Brüderstraße 34, 04103 Leipzig, Germany ²Helmholtz Institute for Metabolic, Obesity, and Vascular Research (HI-MAG) of the Helmholtz Zentrum München at the University of Leipzig and University Hospital Leipzig, Ph.-Rosenthal-Str. 27, 04103 Leipzig, Germany ³Department of Medicine, University of Leipzig, Liebigstraße 20, 04103 Leipzig, Germany

*Corresponding author. E-mail: abeck-sickinger@uni-leipzig.de (A.G. Beck-Sickinger).

***Corresponding author. Helmholtz Institute for Metabolic, Obesity, and Vascular Research (HI-MAG) of the Helmholtz Zentrum München at the University of Leipzig and University Hospital Leipzig, Ph.-Rosenthal-Str. 27, 04103 Leipzig, Germany. E-mail: matthias.blueher@medizin.uni-leipzig.de (M. Blüher).

**Corresponding author. E-mails: nora.kloeting@medizin.uni-leipzig.de, nora.kloeting@helmholtz-muenchen.de (N. Klötting).

Abbreviations: T2D, type 2 diabetes; PPAR α/γ , peroxisome proliferator-activated receptor alpha/gamma; GPCR, G protein-coupled receptor; NPY₁R, neuropeptide Y₁ receptor; NPY, neuropeptide Y; tesa, tesaglitazar; tesa-NPY, [K⁴(GFLG-tesa), F⁷, P³⁴]-NPY; Fapb4, fatty acid binding protein 4; FFA, free fatty acids; Cidec, cell death-inducing DEFA-like effector c; Mcp-1, monocyte chemoattractant protein 1

Received July 26, 2019 • Revision received October 31, 2019 • Accepted November 10, 2019 • Available online 16 November 2019

<https://doi.org/10.1016/j.molmet.2019.11.009>

increased cardiovascular risk, cancer, or weight gain, which lead to complications in clinical trials and restrictions on their use (<https://www.fda.gov/drugs/drug-safety-and-availability/fda-drug-safety-communication-avandia-rosiglitazone-labels-now-contain-updated-information-about> and <https://www.fda.gov/drugs/drug-safety-and-availability/fda-drug-safety-communication-updated-drug-labels-pioglitazone-contain-g-medicines>) [15–19]. Experiments with lipodystrophic mice demonstrated that organs other than adipose tissue mainly contribute to these side effects [20]. Therefore, the selective targeting of PPAR γ agonists to adipocytes represents a promising strategy for the development of safer insulin-sensitizing drugs and is needed to further use these agents in clinics.

Peptide ligands of G protein-coupled receptors (GPCR) are promising targeting moieties for selective cell delivery as they bind with high selectivity and affinity to their receptors, can easily be modified by chemical synthesis, lack antigenicity, and induce an efficient internalization in the target cell [21–23]. Peptide drug conjugates consist of three parts: a carrier peptide that specifically binds to the GPCR expressed on the targeted tissue, a cleavable linker that possesses extracellular stability and is cleaved after translocation to an intracellular compartment, and the drug molecule [24,25]. After activation of the GPCR, the peptide-receptor complex undergoes internalization, which is crucial for delivering the drug inside the cell. The internalized complex is then transferred to the endosome where the linker can be cleaved [26]. This leads to a free drug that can act on either a metabolic or transcriptional level to modulate cell behavior and activity. High levels of neuropeptide Y $_1$ receptor (NPY $_1$ R) mRNA and protein were detected in human adipose tissue, 3T3-L1 preadipocytes, and adipocytes [27–29]. This expression was higher in obese patients [30]. In addition to adipose tissue, NPY $_1$ R can be found in vascular smooth muscle cells and the CNS, including the thalamus, hippocampus, and cerebral cortex [31–33]. Peptide ligand NPY (neuropeptide Y) can cross the blood–brain barrier in rats. However, it is unclear whether this is also the case in humans, as different studies demonstrated that the permeability is low [34–36]. Thus, NPY $_1$ R is a promising target for selective targeting of adipocytes. NPY stimulation of adipocytes leads to a mitogenic effect and enhanced cell proliferation [37,38]. In addition, a high dose of NPY promotes adipocyte differentiation via enhanced PPAR γ expression, which might lead to additional beneficial effects and a combinatorial therapeutic approach of the peptide carrier and drugs [39].

Thiazolidinediones are the most well-known and frequently used class of PPAR γ agonists, yet these molecules do not possess functional moieties suitable for attachment to peptides and therefore cannot be used in peptide drug conjugates [40]. The dual PPAR α/γ agonist tesaglitazar (tesa), in contrast, contains a carboxyl function suitable for synthesis. This agonist is a promising anti-diabetic drug that was already shown to reduce insulin resistance in mice and humans [41–43]. The clinical investigation of tesa was discontinued in phase III because of safety concerns regarding renal dysfunction [16,44]. As these side effects were caused by the action of tesa on the kidney, a selective targeting of tesa to adipocytes could be a promising strategy to continue its clinical trials [45,46]. The advantage of dual PPAR α/γ agonists is, that they, in addition to the insulin-sensitizing effects of PPAR γ , improve lipid parameters and reduce cardiovascular complications associated with metabolic disorders through PPAR α [16,47]. However, these effects are mainly mediated by PPAR α expressed in the kidney, liver, muscle, and endothelial cells [16,45,48]. Therefore, we did not anticipate cardioprotective effects when tesa was selectively targeted to adipocytes and focused on PPAR γ activity in the present study.

In this study, we aimed to transport tesa selectively into adipocytes by targeting it to NPY $_1$ R to develop a safe anti-diabetic drug that combines

the beneficial effects of [F^7 , P^{34}]-NPY and a dual PPAR α/γ agonist while omitting adverse effects in other tissues (Figure 1). Therefore, we synthesized a peptide drug conjugate consisting of NPY $_1$ R-preferring ligand [F^7 , P^{34}]-NPY, a cleavable GFLG linker, and tesa and tested this conjugate extensively in cell culture and *db/db* mice to determine its anti-diabetic potential.

2. MATERIALS AND METHODS

2.1. Materials

To synthesize peptides, N_α -9-fluorenylmethoxycarbonyl (Fmoc)- and *tert*-butyloxycarbonyl (Boc)-protected amino acids were purchased from Orpegen (Heidelberg, Germany) and Iris Biotech (Marktredwitz, Germany). Rink amide resin, 1-hydroxybenzotriazole (HOBT), 2-cyano-2-(hydroxyimino) acetic acid ethyl ester (Oxyma), and N,N' -diisopropylcarbodiimide (DIC) were obtained from Iris Biotech. Thioanisole (TA) and ethanedithiol (EDT) were acquired from Fluka (Buchs, Switzerland). Acetonitrile (ACN), dichloromethane (DCM), and N,N' -dimethylformamide (DMF) were obtained from Biosolve (Valkenwaard, the Netherlands). Diethyl ether and ethanol were purchased from Scharlau (Barcelona, Spain). Hydrazine, piperidine, and trifluoroacetic acid (TFA) were purchased from Sigma Aldrich. For cell cultures and cell culture-related assays, DMEM High Glucose and Ham's F12 cell culture media, Hanks' Balanced Salt Solution (HBSS), Dulbecco's Phosphate-Buffered Saline (DPBS), trypsin–EDTA, and an AdipoRed Adipogenesis Assay Kit were obtained from Lonza (Basel, Switzerland). Fetal calf serum (FCS) was purchased from Biochrom GmbH (Berlin, Germany). Penicillin, streptomycin, and hygromycin B were acquired from Invivogen (Toulouse, France). Biotin, pantothenate, dexamethasone (dex), triiodo-L-thyronine, human apotransferrin, hydrocortisone, dimethyl sulfoxide (DMSO), probenecid, 4-(2-hydroxyethyl)-1-piperazineethanesulfonic acid buffer (HEPES), and Hoechst 33342 were obtained from Sigma–Aldrich (Taufkirchen, Germany). 3-isobutyl-1-methylxanthine (IBMX) was acquired from Fluka (St. Louis, MO, USA) and human insulin was obtained from Roche (Basel, Switzerland). Tesaglitazar, rosiglitazone, and tumor necrosis factor α (TNF α) were purchased from Biomol (Hamburg, Germany). Fluo2-AM and pluronic acid F-127 were acquired from TEF Labs (Austin, TX, USA). OptiMEM was obtained from Life Technologies (Basel, Switzerland). Lipofectamine 2000 and PowerSYBR Green were purchased from Thermo Fischer Scientific (Waltham, MA, USA). A Signal PPAR γ Reporter (luc) Kit, RNeasy Mini Kit, and QuantiNova Reverse Transcription Kit were obtained from Qiagen (Hilden, Germany) and the Dual-Luciferase System Kit from Promega (Madison, WI, USA). Six-well plates and 96-well plates were purchased from TPP AG (Trasadingen, Switzerland), and 8-well μ -slides were obtained from ibidi GmbH (Planegg, Germany).

2.2. Solid phase peptide synthesis (SPPS)

All the peptides were synthesized via a combination of automated solid-phase peptide synthesis (SPPS) with a Syro I peptide synthesizer (MultiSynTech) and manual couplings using the orthogonal Fmoc/*t*Bu strategy on Rink amide resin (15 μ mol scale, loading 0.7 mmol/g). Unmodified NPY (1), [F^7 , P^{34}]-NPY (2), and Boc-[K^4 (Dde), F^7 , P^{34}]-NPY were obtained by robot-assisted synthesis. Coupling reactions were then carried out twice with 8 eq N_α -protected amino acids, in situ activated with equimolar amounts of Oxyma (2 min pre-incubation on resin) and DIC in DMF for 30 min. *Tert*-butyl (*t*Bu for Tyr, Ser, Asp, Glu, and Thr), trityl (Trt for Asn, Gln, and His), 2,2,4,6,7-pentamethylidihydrobenzofuran-5-sulfonyl (Pbf for Arg), and 4,4-dimethyl-2,6-dioxocyclohex-1-ylidenethyl (Dde for Lys) protection groups were used to protect the reactive side chains of

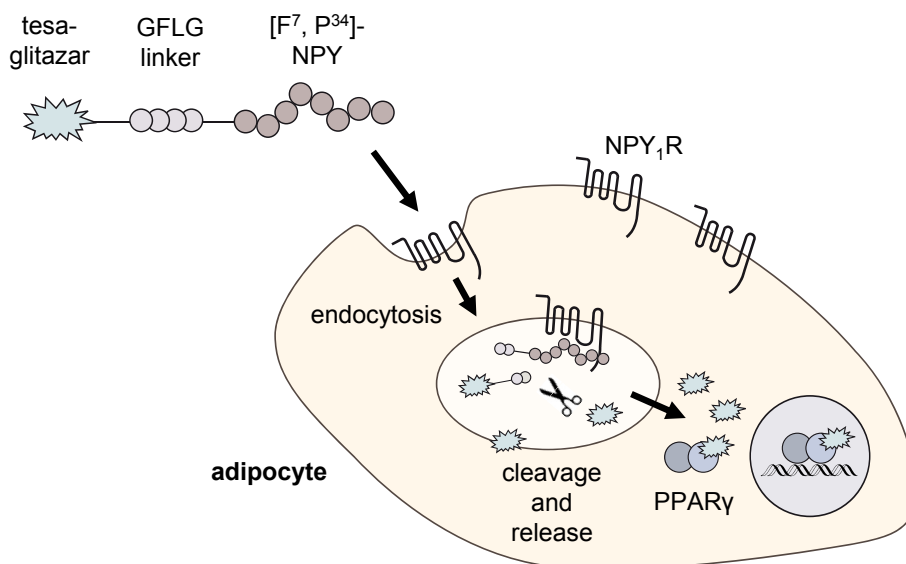


Figure 1: Schematic illustration of adipocyte targeting by peptide drug conjugates. NPY₁R expressed on the adipocyte cell surface can potentially be used for the selective delivery of PPAR γ agonists into adipocytes. The carrier peptide [F^7 , P^{34}]-NPY is conjugated with a cleavable linker and tesa pharmacophore and can bind NPY₁R, thereby triggering activation and subsequent internalization. The peptide-receptor complex undergoes endocytosis into the endosome, where the linker can be cleaved and tesa is released, which activates PPAR γ and thus regulates transcription.

the indicated amino acids. Deprotection of Fmoc was performed automatically with 40% (v/v) piperidine in DMF for 3 min and 20% (v/v) piperidine in DMF for 10 min.

After automated synthesis, deprotection of K^4 (Dde) (Boc- $[K^4$ (Dde), F^7 , P^{34}]-NPY) was conducted 12 times using 2% (v/v) hydrazine in DMF for 10 min. Manual elongation of the N_ϵ -group of K^4 with the amino acids GFLG and the PPAR γ agonist tesa was performed using standard DIC/HOBt activation (5 eq) for coupling and piperidine for Fmoc deprotection to obtain [K^4 (GFLG-tesa), F^7 , P^{34}]-NPY (3).

All of the peptides were cleaved from the resin using TFA/scavenger (9:1 (v/v)) for 3 h, with TA/EDT (7:3, v/v) as a scavenger. The peptides were precipitated with ice cold diethyl ether, washed, and collected by centrifugation. RP-HPLC (Shimadzu) with a Kinetex column was used for peptide purification at a flow rate of 15 ml/min and a linear gradient system containing 0.1% (v/v) TFA in water (eluent A) and 0.08% (v/v) TFA in ACN (eluent B).

Pure products were characterized by analytical RP-HPLC, MALDI-ToF (Ultraflex III, MALDI-ToF/ToF, Bruker Daltonics), and ESI-HCT (high-capacity ion trap ESI-MS, Bruker Daltonics). For RP-HPLC, a LaChromElite system (VWR) with Phenomenex Jupiter Proteo C12 90 Å and Agilent VariTide RPC columns was used with different linear gradients of eluent B (0.08% (v/v) TFA in ACN) in eluent A (0.1% (v/v) TFA in H₂O), detection at 220 nm, and peak integration using EZ Chrome Elite software. The peptides were dissolved in DMSO with a final concentration of less than 0.1% DMSO for all of the in vitro experiments.

2.3. Cell culture

COS-7 (African green monkey kidney) cells stably expressing NPY_{1/2/4/5}R and chimeric G protein ($\Delta 6G\alpha_{q14-myr}$) were cultured in DMEM High Glucose Medium with 10% (v/v) heat inactivated FCS, 100 units/ml penicillin, and 100 μ g/ml streptomycin. HEK293 (human embryonic kidney) cells were grown in DMEM High Glucose Medium and Ham's F12 (1:1 (v/v)) supplemented with 15% (v/v) heat inactivated FCS. HEK293 cells stably expressing NPY_{1/2/4/5}R C-terminally fused to eYFP were maintained in DMEM High Glucose Medium and Ham's F12 (1:1 (v/v))

supplemented with 15% (v/v) heat inactivated FCS and 100 μ g/ml hygromycin B. 3T3-L1 (murine fibroblast) cells were grown in DMEM High Glucose Medium and 10% (v/v) not-heat inactivated FCS. The 3T3-L1 cells were split every second day to avoid confluency. SGBS (human fibroblast) cells were cultivated in DMEM High Glucose Medium and Ham's F12 (1:1 (v/v)) supplemented with 15% (v/v) not-heat inactivated FCS, 8 mg/l biotin and 4 mg/l pantothenate. The SGBS cells were split every third day to avoid confluency. All of the cell lines were maintained under a humidified atmosphere at 37 °C and 5% CO₂.

2.4. Y-receptor activation studies

Signal transduction Ca²⁺-flux assays were performed as previously described [49]. Briefly, COS-7 cells stably expressing NPY_{1/2/4/5}R and chimeric G protein ($\Delta 6G\alpha_{q14-myr}$) were seeded into black 96-well plates and grown for 24 h. The cells were incubated with 0.01% (v/v) Pluronic Acid F-127 and 2.4 μ M Fluo2-AM in assay buffer (HBSS, 1.25 mM Probenecid, and 20 mM HEPES) at 37 °C for 60 min. A one-addition protocol of FlexStation 3 (Molecular Devices, San Jose, CA, USA) was used to perform fluorescent detection (excitation: 485 nm, emission: 525 nm). Indicated concentrations of peptides were added after a 20 s baseline recording, followed by 80 s detection of Ca²⁺ efflux. The signal response was quantified as x-fold over basal and normalized to the maximum response of the native ligand NPY (NPY_{1/2/5}R) or hPP (NPY₄R) set to 100%. The values were calculated using GraphPad Prism 5.0 via non-linear regression and represented the total mean \pm SEM of the EC₅₀ determined in $n \geq 2$ independent experiments each performed in duplicate. The pEC₅₀ \pm SEM values corresponded to the negative decadic logarithm of the EC₅₀ value.

2.5. Live cell microscopy

Y-receptor internalization was investigated as previously described [50]. Briefly, HEK293 cells stably expressing NPY_{1/2/4/5}R C-terminally fused to eYFP were seeded into 8-well μ -slides and allowed to attach for 24 h. The cells were starved in Opti-MEM reduced serum medium (containing 100 μ g/ml CHX and 6 μ g/ml BFA)

supplemented with Hoechst 33342 nuclear stain (0.5 mg/ml) at 37 °C for 30 min. The cells were then stimulated with 100 nM of peptide at 37 °C for 60 min and washed with acidic wash solution and HBSS. To visualize the peptide uptake, the cells were incubated with 100 nM TAMRA labeled [K4(GFLG-TAMRA), F⁷, P³⁴]-NPY for 10 min, followed by an acidic wash (50 mM glycine, 180 mM NaCl, and pH 3.1) to remove the excess labeled peptide, washed in HBSS, and returned to the Opti-MEM. Microscopy images were taken using an Axio Observer microscope equipped with an ApoTome imaging system and a Heating Insert P Lab-Tek S1 unit (Zeiss, Oberkochen, Germany). Image editing was performed with AxioVision software version 4.6. The assays were performed in at least two independent experiments.

2.6. PPAR reporter gene assay

HEK293 cells stably expressing NPY₁R C-terminally fused to eYFP were seeded into white 96-well plates, grown to 70–80% confluence, and transfected using Lipofectamine 2000 transfection reagent according to the manufacturer's protocol. For luciferase reporter gene assays, 250 ng reporter plasmid, positive control plasmid or negative control plasmid (Cignal PPAR Reporter (luc) Kit), 250 ng PPAR γ expression vector, and 250 ng RXR α expression vector were applied in addition to 0.75 μ l of Lipofectamine 2000 transfection reagent per well. For selectivity assays, HEK293 cells without stable NPY₁R-eYFP transfection and HEK293 NPY₁R-eYFP cells without PPAR γ transfection were used. After 24 h of transfection, the cells were treated with tesa or peptides for an additional 24 h. For competition assays, the cells were treated with a 20-fold concentration of NPY simultaneous to peptide stimulation. Luciferase assays were performed using the Dual-Luciferase System Kit according to the manufacturer's instructions. The relative firefly luciferase activity was normalized by the corresponding Renilla luciferase activity, the luciferase activity of the cells transfected with the negative control plasmid, and the DMSO vehicle control. The assays were performed in at least three independent experiments.

2.7. Differentiation and AdipoRed assay of 3T3-L1 and SGBS cells

3T3-L1 or SGBS cells were seeded into 96-well plates and grown to complete confluency (set as day 0). On day 2 of confluence, the 3T3-L1 cells were differentiated by DMEM High Glucose Medium supplemented with 10% (v/v) not-heat inactivated FCS, 0.5 mM IBMX, 167 nM human insulin, and 1 μ M dexamethasone (differentiation medium). On day 4, the medium was replaced by insulin medium (DMEM High Glucose Medium, 10% not-heat inactivated FCS, and 167 nM human insulin). On day 6, the medium was changed to standard culture medium and changed every other day until full differentiation was achieved (on day 8). The SGBS cells were differentiated as previously described [51]. Briefly, DMEM High Glucose Medium and Hams F12 (1:1 (v/v)) without FCS, supplemented with 0.01 mg human apo-transferrin, 20 nM human insulin, triiodo-L-thyronine, 100 nM hydrocortisone, 25 nM dexamethasone, 0.5 mM IBMX, and 2 μ M rosiglitazone (quick differentiation medium, QD) was added on day 0. On day 4, the medium was replaced by 3FC medium (DMEM High Glucose Medium and Hams F12 (1:1 (v/v))) without FCS and supplemented with 0.01 mg human apo-transferrin, 20 nM human insulin, triiodo-L-thyronine, and 100 nM hydrocortisone. The medium was changed every second day until full differentiation was achieved (day 10).

On day 2 of the 3T3-L1 or SGBS differentiation process, tesa or peptides were added to the differentiation or QD medium at the indicated concentrations. For the SGBS, QD medium without rosiglitazone

was used. After 24 h, differentiation was continued as previously described. To determine the intracellular triglyceride content as an indicator of adipocyte differentiation, the AdipoRed Adipogenesis Assay was performed according to the manufacturer's protocol. Fluorescence (excitation: 485 nm, emission: 572 nm) was measured with an Infinite 200 microplate reader (Tecan Group, Männedorf, Switzerland). For normalization, the relative differentiation was calculated as the DMSO vehicle control was set to 100%. Three independent experiments with four replicates were conducted.

2.8. qRT-PCR

The 3T3-L1 or SGBS cells were seeded into 6-well plates and differentiated as previously described. Tesa or peptides were added to the differentiation medium at a concentration of 100 μ M on day 2, followed by 12 h or 24 h incubation. On day 4, the cells were washed two times with PBS, harvested by trypsinization, and stored at -70 °C until RNA isolation was performed. RNA extraction was performed using the RNeasy Mini Kit or TRIzol (Life Technologies, Grand Island, NY, USA), followed by reverse transcription with standard reagents (Life Technologies, Grand Island, NY, USA) or the QuantiNova Reverse Transcription Kit. qRT-PCR was performed with QuantiTect Primer Assays (Qiagen, Hilden, Germany) or TaqMan Gene Expression Assays (Thermo Fischer Scientific, Waltham, MA, USA: 36B4 #MM00725448, 18sRNA #Hs99999901, Fabp4 #MM00445878, adiponectin #MM00456425, and PPAR-gamma #MM00440940) using a Power SYBR Green or Brilliant SYBR Green QPCR Core Reagent Kit from Stratagene (La Jolla, CA, USA) according to the manufacturer's instructions on an Applied Biosystems 7500 Real-Time PCR or comparable system (Applied Biosystems, Foster City, CA, USA). $N \geq 3$ independent experiments with two replicates were performed. For the cell culture experiments, the data were analyzed according to the $2^{-\Delta\Delta Ct}$ method using 36B4 or GAPDH as housekeeping genes and DMSO treatment as a control. Liver mRNA expression was calculated relative to 18sRNA, which was used as an internal control due to its resistance to glucose-dependent regulation [52]. The mRNA levels were quantified using the standard curve method of QuantStudio 6 Flex software (Applied Biosystems, Foster City, CA, USA), determining the crossing points of the individual samples using an algorithm that identifies the first turning point of the fluorescence curve. Amplification of the specific transcripts was confirmed by the melting curve profiles (cooling the sample to 68 °C and heating slowly to 95 °C while measuring the fluorescence) at the end of each PCR [53].

2.9. Animal studies

All of the experiments were performed according to the animal ethical laws of the state Saxony, Germany, and were approved by the local animal ethics review board (Landesdirektion Sachsen, Leipzig, Germany). Female *db/db* mice 12–15 weeks of age were purchased from Taconic (Denmark) and housed in groups of 5 in temperature- and humidity-controlled facilities in a 12 h:12 h light–dark cycle and had free access to tap water and food (regular chow, Sniff, Soest, Germany). Three out of seven groups served as controls ($N = 15$, see Table 1). The 5 *db/db* mice were untreated and 10 *db/db* mice were vehicle treated either orally or intraperitoneally (i.p.). One additional group ($n = 5$) of lean C57BL/6NTac mice was used as a metabolically healthy control group. Groups 1 to 5 were treated daily with 2.5 μ mol/kg body weight tesa, peptides or vehicle (1% (v/v) DMSO in PBS) either by gavage or intraperitoneal injection for 8 days according to Table 1. The control mice were gavaged with an equal volume of vehicle.

Table 1 — Groups of mice that were used for the in vivo Tesa-NPY studies.

Group	Mice	Treatment	Administration
1 (n = 5)	<i>db/db</i>	Tesa	Oral
2 (n = 5)	<i>db/db</i>	Tesa-NPY (3)	Intraperitoneal
3 (n = 5)	<i>db/db</i>	[F ⁷ , P ³⁴]-NPY (2)	Intraperitoneal
4 (n = 5)	<i>db/db</i>	Vehicle control	Oral
5 (n = 5)	<i>db/db</i>	Vehicle control	Intraperitoneal
6 (n = 5)	<i>db/db</i>	Untreated control	—
7 (n = 5)	C57BL/6N	Untreated healthy	—

2.10. Phenotypical characterization

All of the mice were monitored for 9 days during the treatment period. Body weight, food intake, and water uptake were recorded daily and body composition (lean body mass and whole body fat mass) was recorded at the beginning, middle, and end of the study in the conscious mice using an EchoMRI system (Echo Medical Systems, Houston, TX, USA). At the beginning and end of the treatment period, the HbA1c levels were determined from 5 μ l of whole venous blood samples using an automated chemical analyzer at the Institute of Laboratory Medicine and Clinical Chemistry and beta-ketone using an automated glucose monitor (FreeStyle Precision H, Abbott GmbH, Ludwigshafen, Germany). Rectal body temperature was measured once on day 9 using Thermalert (TH-5, Physitemp, Clifton, NJ, USA). The mice were sacrificed on day 9 via an overdose of anesthetic (isoflurane, Baxter, Unterschleißheim, Germany). Subcutaneous (sc) and epigonadal (epi) adipose tissue (AT) was immediately removed and frozen in liquid nitrogen. Serum was collected for measurements of triglycerides (TG), free fatty acid (FFA), cholesterol, insulin, adiponectin, leptin, and monocyte chemoattractant protein 1 (Mcp-1).

2.11. Serum parameter analysis

Serum insulin (mouse insulin ELISA, Mercodia, Uppsala, Sweden), adiponectin (mouse adiponectin ELISA, AdipoGen, San Diego, CA, USA), leptin (mouse leptin ELISA, Crystal Chem, Downers Grove, IL, USA), and Mcp-1 (mouse/rat CCL2/JE/Mcp-1 Quantikine ELISA, R&D Systems, Minneapolis, MN, USA) levels were analyzed via ELISA according to the manufacturer's instructions. Serum concentrations of TG, FFA, and cholesterol were measured by an automatic chemical analyzer at the Institute of Laboratory Medicine and Clinical Chemistry.

2.12. Histology and adipocyte size measurements

Subcutaneous AT and epigonadal AT were fixed, paraffin embedded, sectioned (5 μ m), and H&E stained as previously described [54]. Microscopy images were taken using an Axio Observer microscope (Zeiss, Oberkochen, Germany). The adipocyte size was analyzed from at least 50 cells per slice using AxioVision software version 4.6.

2.13. Microarray experiments and analyses

Transcriptome profiling was performed in epigonadal samples from 3 mice from each experimental group using a mouse Clariom S Assay from Affymetrix. The RNA integrity and concentration, RNA hybridization, scanning procedures, and post-processing were performed according to Affymetrix's protocol at our genetic technologies core unit. An expression matrix from the Affymetrix data was created using the robust multi-array average algorithm (RMA) in RMAExpress [55]. Briefly, the raw intensity values were background corrected, log₂ transformed, and then quantile normalized. A linear model was then fit to the normalized data to obtain the expression measurements for each probe set on each array. Mapping of the manufacturer's Probe ID to

data from public repositories (ENTREZ gene identifiers and ENSEMBL accession numbers) was performed using annotation packages available from Bioconductor version 3.7 (MacDonald JW (2017) *clariomsmousetranscriptcluster.db*: Affymetrix clariomsmouse annotation data (chip clariomsmousetranscriptcluster) using R package version 8.7.0). Gene expression data were analyzed using the R statistical environment (R Core Team (2017), R Foundation for Statistical Computing, Vienna, Austria, <https://www.R-project.org>). Log₂-transformed values were analyzed using the Bayesian moderated t-statistic implemented in the limma package version 3.32.10 [56]. The linear model was fit to a design matrix including treatment as a factor variable with 2 levels and a "toptable" was produced with information on the fold changes in the gene expression according to the treatment, corresponding p-values, and multiple testing adjusted p-values according to the Benjamini-Hochberg procedure.

Gene ontology enrichment analysis for processes, functions, and components was performed using the Gene Ontology enrichment analysis and visualization tool (GORilla) [57]. KEGG pathways and gene ontology (GO) gene sets were generated using *kegg.gsets*, *go.gsets*, and *gageData*. KEGG pathways were plotted using the Pathview package [58]. The figures were produced using the ggplot2 package [59], Pheatmap (Raivo Kolde (2016), Pheatmap: Pretty Heatmaps, R package version 1.0.9.), and REVIGO [60].

2.14. Statistical analysis

Statistical analysis was performed using GraphPad Prism 5.03 (GraphPad Software, Inc., San Diego, CA, USA). Statistical significance was determined via one-way analysis of variance (ANOVA) followed by Dunnett's multiple comparison test for the cell culture studies and the non-parametric Mann-Whitney U-test for the animal studies. Statistical analyses for microarray data were previously described.

3. RESULTS

3.1. Peptide synthesis of Tesa-NPY

Unmodified NPY (1) and NPY₁R-preferring ligands [F⁷, P³⁴]-NPY (2) were synthesized by automated solid phase peptide synthesis (SPPS) using the orthogonal Fmoc/tBu strategy [61]. For [K⁴(GFLG-tesa), F⁷, P³⁴]-NPY (tesa-NPY) (3), a combination of automated SPPS and manual couplings was used. Tesa was then linked to [F⁷, P³⁴]-NPY (2) by an enzymatically cleavable GFLG linker (Figure 2).

Previous studies demonstrated that modifications at position 4 of NPY do not change the peptide's activation and internalization behavior [62–64]. Modification of the *N*_ε group of Lys⁴ was achieved by the selective hydrazine-induced removal of the orthogonal Dde protecting group and the subsequent attachment of the GFLG linker and tesa via standard DIC/HOBt coupling. After cleavage from the Rink amide resin, all of the peptides were purified by RP-HPLC to a purity of >95%. The identity and purity of the peptides were confirmed by MALDI-ToF, ESI-HCT mass spectrometry, and analytical RP-HPLC (Table 2). The analytical data for tesa-NPY (3) are shown in Figure 3.

3.2. Tesa-NPY is a potent NPY₁R agonist and induces NPY₁R internalization

The receptor activation, selectivity, and internalization were investigated to ensure that the attachment of the cleavable linker and tesa did not alter the behavior of NPY₁R-preferring carrier peptide [F⁷, P³⁴]-NPY. The activation of the human Y-receptors was tested using Ca²⁺-flux assays in COS-7 cells stably expressing one specific Y-receptor subtype (NPY_{1/2/4/5}R) and chimeric G protein (Δ 6G $\alpha_{q14-myr}$), opening

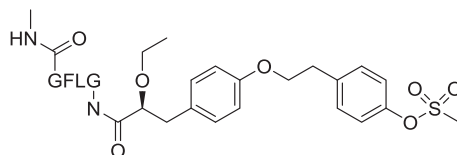
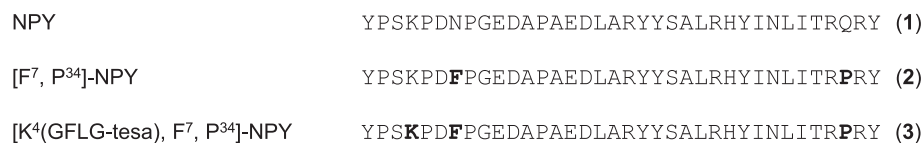


Figure 2: Sequences and structures of peptides. Peptide sequences of NPY (1), [F⁷, P³⁴]-NPY (2), and [K⁴(GFLG-tesa), F⁷, P³⁴]-NPY (3). Chemical structures of the PPAR α / γ agonist tesa and the cleavable GFLG linker used to attach tesa to the peptide.

No.	Compound	MALDI-ToF MS		ESI	RP-HPLC retention time (min)		Purity (%)
		M _{calc.} (Da)	M _{obs.} (M + H) ⁺	M _{obs.} (z) (Da)	Column A	Column B	
(1)	NPY	4251.1	4252.0	1064.3 (4+) 851.6 (5+) 709.8 (6+) 608.5 (7+)	22.0 (20-60-40)	18.7 (20-60-40)	>95
(2)	[F ⁷ , P ³⁴]-NPY	4253.1	4254.0	1064.9 (4+) 852.0 (5+) 710.9 (6+) 609.0 (7+)	23.3 (20-60-40)	19.8 (20-60-40)	>95
(3)	[K ⁴ (GFLG-tesa), F ⁷ , P ³⁴]-NPY	5017.5	5018.5	1256.1 (4+) 1005.0 (5+) 837.7 (6+) 718.1 (7+)	20.5 (30-60-30)	19.5 (30-60-30)	>95

the Ca²⁺ channels upon receptor activation (Figure 4A-D, Table 3) [49,65].

Tesa-NPY (3) is a potent NPY₁R agonist as indicated by EC₅₀ values comparable to that of carrier peptide [F⁷, P³⁴]-NPY (2) and native ligand NPY (1). At NPY₂R, a 400-fold loss in the tesa-NPY (3) activity was observed compared to NPY (1), which was even higher than the 160-fold loss of NPY₁R-preferring [F⁷, P³⁴]-NPY (2). These data demonstrate the strong NPY₁R selectivity of the peptide-drug conjugate toward NPY₂R. The activity of [F⁷, P³⁴]-NPY (2) at NPY₄R and NPY₅R was comparable to the activity of the native ligands hPP (NPY₄R) and NPY (NPY₅R) (1). This limited selectivity of [F⁷, P³⁴]-NPY toward NPY₄R and NPY₅R was previously detected during its development [54,58]. However, the modification of [F⁷, P³⁴]-NPY with tesa led to a strong loss of activity (25-fold) at the NPY₄R subtype and a slight loss of activity at NPY₅R. These results demonstrate that the tesa-modified [F⁷, P³⁴]-NPY (3) was more NPY₁R selective than the unmodified [F⁷, P³⁴]-NPY (2), especially with respect to the effects at NPY₄R.

The selectivity of tesa-NPY (3) was further investigated by live cell imaging of ligand-induced Y-receptor internalization using a HEK293 cell line that stably expresses NPY_{1/2/4/5}R-eYFP fusion protein (Figure 4E). The receptors (yellow) were mainly present in the membrane prior to stimulation and only minor fluorescence was detected in the intracellular compartments, which was caused by overexpression in the stable cell lines and due to the accumulation of receptor proteins in the endoplasmic reticulum and Golgi apparatus [62,66,67]. Because we observed continuous replenishment of membrane-localized NPY₁R and NPY₄R receptors during internalization, we added translation inhibitor CHX and ER-Golgi transport inhibitor BFA to the medium to facilitate the detection of reduced receptor localization to the

membrane upon internalization. The native ligand NPY (1) and peptide conjugate tesa-NPY (3) induced NPY₁R internalization as indicated by an increase in the yellow fluorescence in the intracellular vesicles and a decrease in the membrane fluorescence. For NPY₂R and NPY₄R, only the native ligands NPY (NPY₂R)/hPP (NPY₄R) induced an internalization, whereas stimulation with tesa-NPY (3) led to only minor endocytosis. For NPY₅R, it was previously described that internalization occurs much slower and in a lower amount than for the other Y-receptor subtypes, which was also detected in the present study [68]. To confirm these findings, we incubated the cells with fluorescently labeled [K⁴(GFLG-TAMRA), F⁷, P³⁴]-NPY and monitored the uptake of red fluorescent linker peptide used to shuttle tesa preferably to NPY₁R-expressing cells.

These results demonstrated that NPY₁R activity and the preference of tesa-NPY (2) over NPY₂R and NPY₄R was even higher than that of unmodified [F⁷, P³⁴]-NPY (3). Selectivity toward NPY₅R can be ensured as this receptor undergoes only minor endocytosis.

3.3. Tesa-NPY induces PPAR γ transcriptional activity in cells expressing NPY₁R and PPAR γ

To examine whether the tesa-NPY conjugate (3) was able to activate the PPAR γ nuclear receptor, HEK293 cells stably expressing NPY₁R were transfected with a plasmid-expressing luciferase under the control of the PPAR-responsive element PPRE. Furthermore, plasmids coding for PPAR γ and RXR α were transfected. Because PPAR γ binds as a heterodimer with RXR α to PPRE-responsive elements, RXR α is needed for PPAR γ activity [40]. After transfection, the cells were treated with free tesa, carrier peptide [F⁷, P³⁴]-NPY (2), or the tesa-NPY conjugate (3) and the luciferase activity was measured (Figure 5).

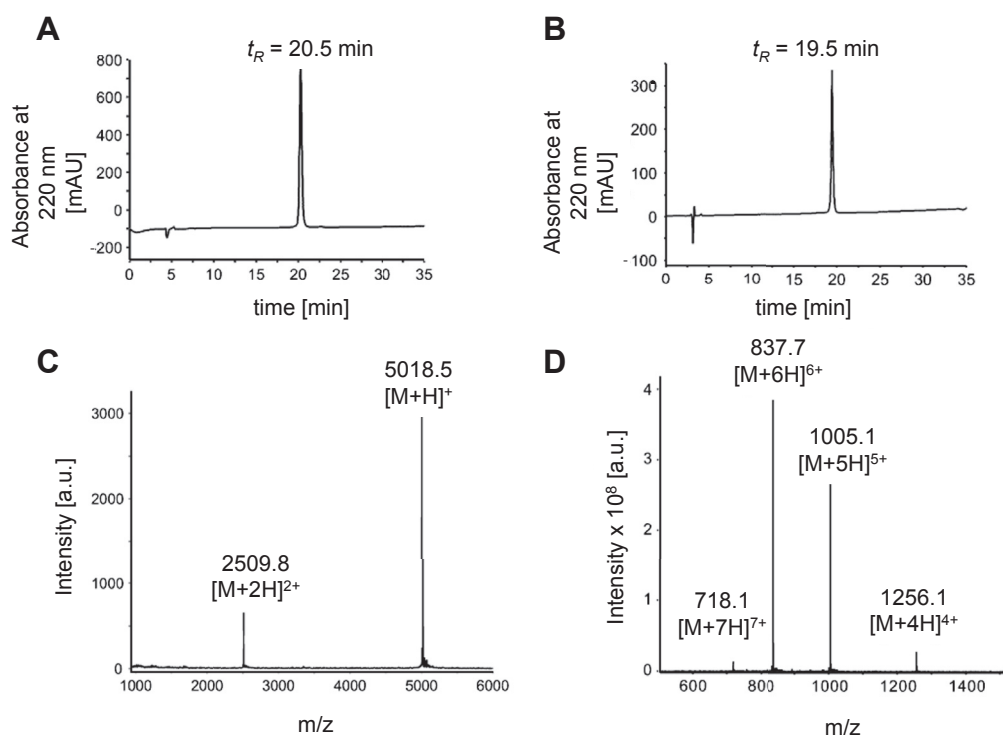


Figure 3: Analytical data of [K⁴(GFLG-tesa), F⁷, P³⁴]-NPY (3). (A) Analytical RP-HPLC using a Phenomenex Jupiter Proteo C12 90 Å column and (B) an Agilent VariTide RPC column with a linear gradient of 30–60% (v/v) ACN/H₂O in 30 min. (C) MALDI-ToF mass spectrum showing the single- and double-loaded molecule ion signals ($M_{\text{calc.}} = 5017.5$ Da). (D) ESI mass spectrum displaying the four-, five-, six-, and seven-fold charged molecule ions. t_R = retention time, AU = absorption units, a.u. = arbitrary units.

Concentration-dependent luciferase activity was detected in the tesa and tesa-NPY (3) treated cells (Figure 5A). [F⁷, P³⁴]-NPY (2), in contrast, did not contain a PPAR γ agonist and was thus unable to induce transcriptional activity. However, the free tesa demonstrated a saturation curve, whereas saturation was not achieved for the tesa-NPY (3). Most likely, higher concentrations of the drug are needed for comparable effects. However, with respect to higher concentrations, the assay is technically limited due to the peptide's solubility. The peptide's lower potency was likely due to the selective transport and release of the peptide conjugate. Whereas free tesa is taken up by the cells through passive diffusion, peptide conjugate needs to be taken up by endocytosis and the drug has to be released. This process is further limited by the receptor expression level on the cell surface. Thus, higher concentrations of peptide conjugate are needed to reach the same concentration inside the cell, as was previously shown for cytotoxic NPY conjugates with comparable size and polarity [63,66]. To confirm that the PPAR γ activity of the tesa-NPY (3) was induced by NPY₁R-mediated internalization, the effect of the conjugate was investigated in the presence of an excess of unmodified NPY₁R agonist (NPY) (Figure 5B). Incubation with NPY alone did not lead to any transcriptional activity, whereas tesa-NPY induced it. Indeed, unlabeled NPY competed with tesa-NPY (3) for binding to NPY₁R and therefore its transcriptional activity, confirming the receptor-mediated mechanism of PPAR γ activation by the peptide-drug conjugate. Further verification of the peptide conjugate specificity was performed using cells that do not express either NPY₁R or PPAR γ (Figure 5C). The activity of the free tesa, taken up by passive diffusion, was not influenced by NPY₁R expression, whereas the absence of PPAR γ led to a complete loss of transcriptional activity (left). In contrast, for the tesa-NPY conjugate (3),

the presence of both the receptor and PPAR γ was mandatory to exert its effects, as expected for receptor-mediated uptake of the compound. In the absence of NPY₁R, the levels dropped to basal levels comparable to unstimulated PPAR γ expressing cells. In the absence of PPAR γ , even the basal levels of transcriptional activity were lost, leading to negative values in the assay. Apparently HEK cells do not express detectable levels of endogenous PPAR proteins that can be activated in the assay.

These results demonstrated that tesa was selectively internalized through [F⁷, P³⁴]-NPY and activated PPAR γ in the cells stably expressing NPY₁R. Next, the activity of tesa-NPY in cells with native NPY₁R expression is addressed.

3.4. Tesa-NPY enhances adipogenesis and the expression of adipocyte-marker genes in 3T3-L1 and SGBS cells

The activation of PPAR γ is sufficient and necessary for adipogenesis [69]. Thus, the tesa-NPY conjugate (3) was analyzed for its ability to stimulate murine 3T3-L1 and human SGBS preadipocyte differentiation into mature adipocytes. This was assessed via quantification of the intracellular triglyceride (TG) content, as adipocytes accumulate TG in response to cell differentiation (Figure 6A-D) [70]. The 3T3-L1 and SGBS cells were differentiated as illustrated in Figure 6A/B. Treatment with 10/25/100 μ M of free tesa and 100 μ M of tesa-NPY (3) enhanced adipogenesis in both cell lines (Figure 6C/D). In contrast, [F⁷, P³⁴]-NPY (2) had no influence on adipocyte differentiation. As previously discussed for the reporter gene assay in HEK cells (Figure 5), higher concentrations (unfeasible due to solubility issues) or longer constant treatment with tesa-NPY (3) is needed to obtain comparable effects as observed for free tesa.

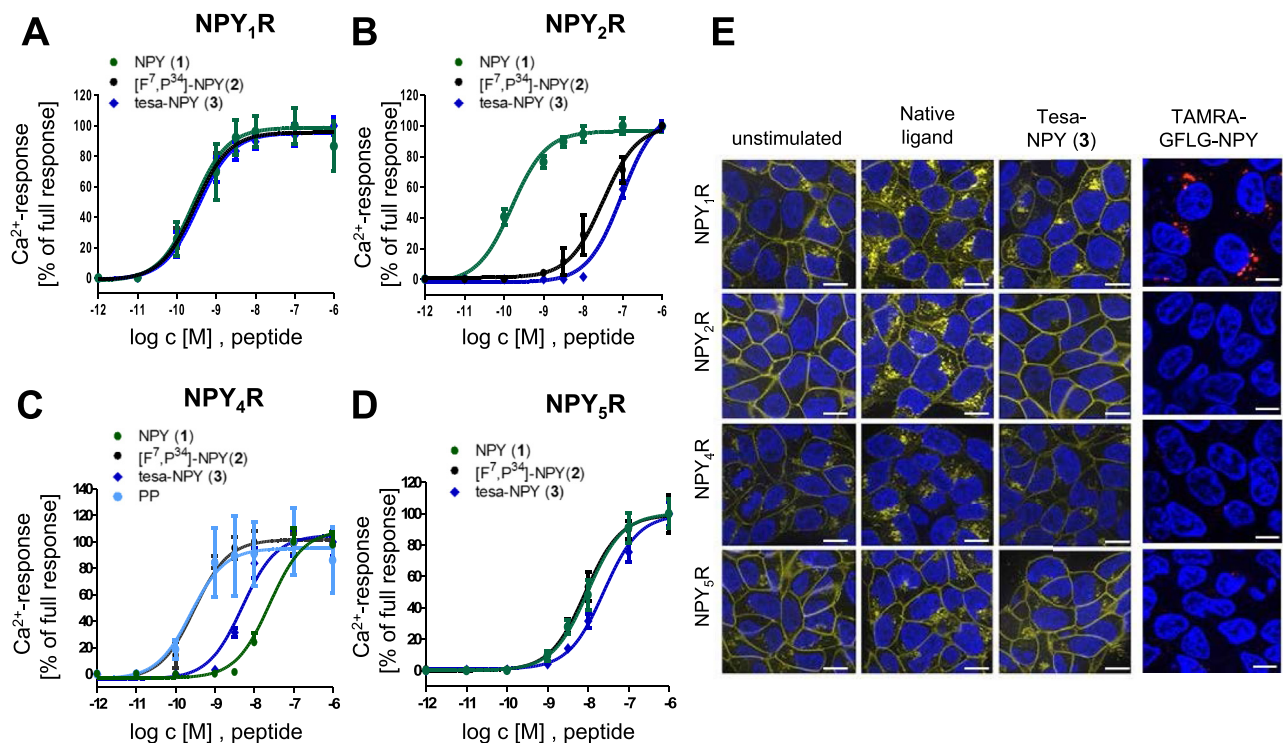


Figure 4: Receptor activation and internalization of peptides. (A–D) Ca²⁺-flux assays in stably transfected COS-7 cells to measure the activity of NPY (1) or hPP, [F⁷, P³⁴]-NPY (2), and tesa-NPY (3) on the respective human Y-receptor subtype NPY₁R (A), NPY₂R (B), NPY₄R (C), NPY₅R (D). The depicted values represent the mean ± SEM from n ≥ 2 independent experiments. Data were normalized to maximum NPY (NPY_{1/2/5}R) or hPP (NPY₄R) response. (E) Receptor internalization of (1) and (3) studied in HEK293 cells stably expressing the respective human Y-receptor subtype fused to eYFP (yellow). Cells were stimulated with 100 nM of peptides for 1 h. Uptake of the fluorescent-labelled linker peptide [K⁴(GFLG-TAMRA), F⁷, P³⁴]-NPY (red) was monitored after incubation for 10 min. Hoechst33342 was used for nuclear staining (blue). Representative pictures from two independent experiments. Scale = 10 μm.

Moreover, PPAR γ activation leads to the expression of several adipogenic markers, such as adiponectin, fatty acid binding protein 4 (Fabp4), and cell death-inducing DEFA-like effector c (Cidec). The expression of these genes in response to tesa-NPY (3) was assessed via qPCR (Figure 6E/F) [71–74]. The 3T3-L1 and SGBS cells were differentiated as previously described, harvested on day 3 or 4, and used for qPCR. The expression of adiponectin in the 3T3-L1 cells was upregulated by the free tesa and peptide conjugate (3), but not for [F⁷, P³⁴]-NPY (2). The expression of Fabp4 and Cidec in the 3T3-L1 cells was enhanced by free tesa, but no significant effect of tesa-NPY (3) and [F⁷, P³⁴]-NPY (2) was visible. In the SGBS cells, tesa and tesa-NPY (3) enhanced the expression of adiponectin, Fabp4, and Cidec. However, only Fabp4 induction by tesa reached significant differences. [F⁷, P³⁴]-NPY (2) showed no effect.

These data point to successful internalization, release, and activity of tesa-NPY (3) in cells natively expressing NPY₁R. Finally, we tested whether the peptide conjugate was active and able to induce anti-diabetic effects in vivo.

3.5. Tesa-NPY influences body weight and adipose tissue morphology in *db/db* mice

The *db/db* mice were treated with 2.5 μM/kg/day tesa, tesa-NPY (3), or [F⁷, P³⁴]-NPY (2) over 8 days. The controls represent the untreated *db/db* mice and the *db/db* mice treated with vehicle (1% (v/v) DMSO in PBS). Changes in body weight during the treatment were measured. The mice treated with tesa and tesa-NPY (3) did not change significantly, whereas their littermates treated with [F⁷, P³⁴]-NPY (2) or vehicle/untreated lost approximately 3% of their body weight (Figure 7A). However, no significant differences between the body composition of the mice (lean mass and fat mass determined by EchoMRI) were detected (Figure 7B/C).

To investigate whether treatment with tesa, tesa-NPY (3), or [F⁷, P³⁴]-NPY (2) affected the adipocyte morphology, the adipose tissue histology was analyzed and the adipocyte size distribution was measured. H&E staining of the subcutaneous and epigonadal adipose tissue depots showed a trend toward smaller epigonadal and subcutaneous cell size in the mice treated with tesa-NPY (3), whereas the mean adipocyte diameter for all of the other mice was comparable (Figure 7D).

3.6. Tesa-NPY influences metabolic parameters in *db/db* mice

In addition to the body weight and body composition, several metabolic parameters were measured after treatment with tesa, tesa-NPY (3), [F⁷, P³⁴]-NPY (2), or vehicle/untreated. The vehicle/untreated *db/db* mice had elevated plasma levels of HbA1C (data not shown), ketone bodies, insulin, and Mcp-1 and reduced plasma levels of adiponectin compared to the lean mice (Figure 8), which is characteristic of these mice. The treatment significantly delayed rapid diabetes progression, which is prototypical for *db/db* mice. Whereas in the vehicle/untreated

Table 3 — Receptor activation of peptides determined via Ca²⁺-flux assay.

No.	Peptide	EC ₅₀ (nM) (pEC ₅₀ ± SEM)			
		NPY ₁ R	NPY ₂ R	NPY ₄ R	NPY ₅ R
(1)	NPY/hPP	0.4 (9.4 ± 0.2)	0.2 (9.8 ± 0.1)	0.2 (9.6 ± 0.4)	9.9 (8.0 ± 0.1)
(2)	[F ⁷ , P ³⁴]-NPY	0.3 (9.5 ± 0.1)	32 (7.5 ± 0.1)	0.3 (9.5 ± 0.1)	8.5 (8.0 ± 0.1)
(3)	tesa-NPY	0.4 (9.4 ± 0.1)	96 (7.0 ± 0.1)	5.0 (8.3 ± 0.1)	25 (7.6 ± 0.1)

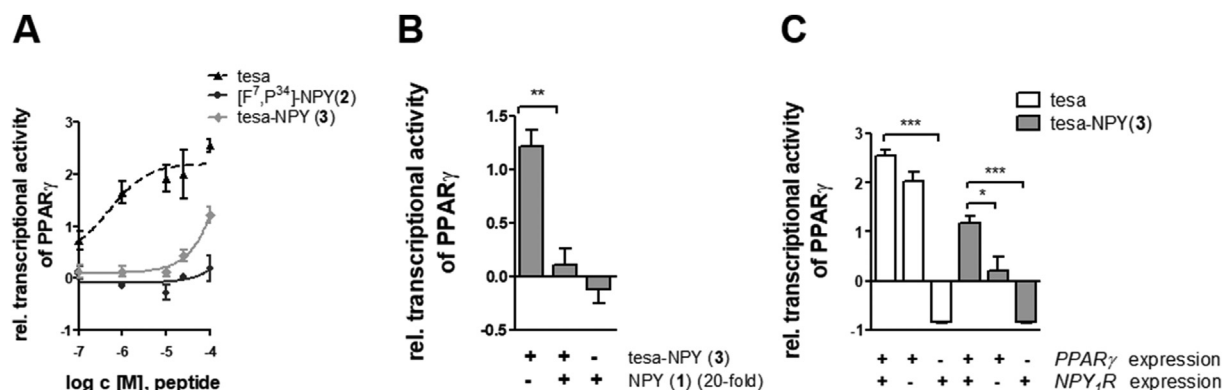


Figure 5: Transcriptional activity of the PPAR reporter gene. (A) Relative transcriptional activity following tesa, $[F^7, P^{34}]$ -NPY (2), or tesa-NPY (3) treatment in HEK293 cells stably expressing NPY_1R , transiently transfected with PPAR reporter gene, $PPAR\gamma$, and $RXR\alpha$ plasmids. (B) Relative transcriptional activity following treatment with 100 μ M tesa-NPY (3) in the presence or absence of 20-fold NPY (1) using HEK293 cells stably expressing the NPY_1R , transiently transfected with the PPAR reporter gene, $PPAR\gamma$ and $RXR\alpha$ plasmids. Treatment with NPY (1) alone served as a negative control. (C) Relative transcriptional activity following treatment with 100 μ M tesa or tesa-NPY (3) in HEK293 cells expressing either NPY_1R or $PPAR\gamma$ or both (in the presence of PPAR reporter gene- and $RXR\alpha$ expression plasmids). The depicted values represent mean \pm SEM from $n \geq 3$ independent experiments. All measurements were normalized to the transcriptional activity of DMSO-treated cells expressing all factors (set to 0). Statistical significance was determined by one-way analysis of variance (ANOVA) followed by Dunnett's multiple comparison test, * ≤ 0.05 , ** $p \leq 0.01$, *** $p \leq 0.001$.

mice, the HbA1C values increased by approximately 2%, a graduated reduced increase was seen for $[F^7, P^{34}]$ -NPY (2), peptide conjugate (3), and tesa (Figure 8A). Body temperature, which decreased to 35 °C in

the vehicle/untreated *db/db* controls, was normalized to 36 °C in all of the treated mice including the mice treated with $[F^7, P^{34}]$ -NPY (2) (Figure 8B). Treatment with tesa and tesa-NPY (3) led to normalization

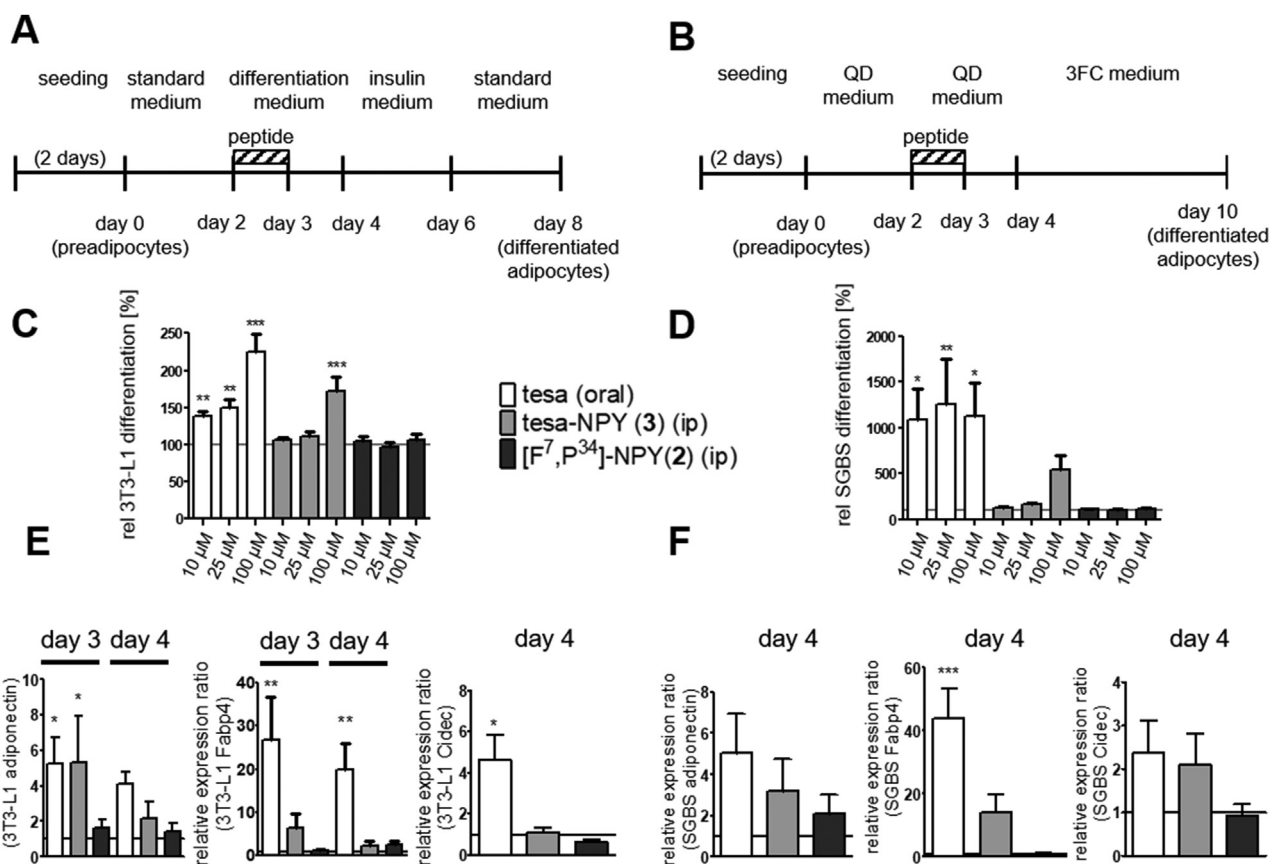


Figure 6: Influence of tesa-NPY (3) on adipogenesis. (A, B) Cells were differentiated and stimulated according to the protocol depicted for 3T3-L1 (A) and for SGBS (B). (C, D) Lipid accumulation was measured by TG staining in differentiated 3T3-L1 (C) or SGBS (D) adipocytes following treatment with indicated concentrations of tesa, $[F^7, P^{34}]$ -NPY (2), or tesa-NPY (3). Bars represent mean \pm SEM from $n = 3$ independent experiments performed in quadruplicates. Measurements were normalized using DMSO (vehicle)-treated cells (set to 100%). Statistical significances refer to vehicle-treated cells. (E, F) Expression of adipocyte-enriched genes in 3T3-L1 (E) or SGBS (F) adipocytes analyzed by qPCR. Values represent mean \pm SEM from $n \geq 3$ independent experiments performed in duplicates. Measurements were normalized according to the $2^{-\Delta\Delta Ct}$ method to 36B4 or GAPDH as housekeeping genes and DMSO-treated cells as control (set to 1). Statistical significances refer to DMSO-treated cells and were determined by one-way analysis of variance (ANOVA) followed by Dunnett's multiple comparison test, * ≤ 0.05 , ** $p \leq 0.01$, *** $p \leq 0.001$.

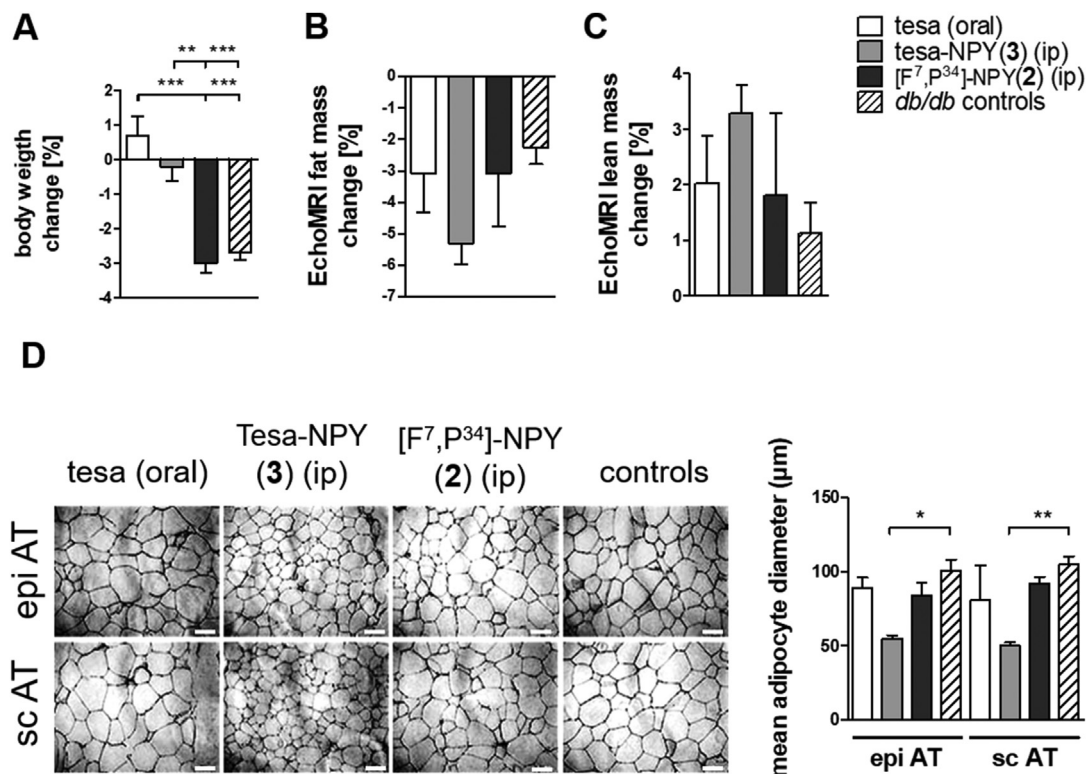


Figure 7: Effects of tesa-NPY (3) on body weight, body composition and adipose tissue morphology in *db/db* mice. (A) Percentage of body weight change over 9 days of mice treated with 2.5 $\mu\text{M}/\text{kg}/\text{day}$ tesa, [F⁷, P³⁴]-NPY (2), or tesa-NPY (3) ($n = 5$). (B, C) The percentage of fat (B) mass and lean (C) mass change determined by EchoMRI over 9 days of mice treated with tesa (2) or tesa-NPY(3) ($n = 5$). Bars represent mean \pm SEM; * ≤ 0.05 , ** ≤ 0.01 , *** ≤ 0.001 determined by one-way analysis of variance (ANOVA) followed by Dunnett's multiple comparison test. D) Adipose tissue morphology determined by H&E staining of epigonadal (epi) and subcutaneous (sc) adipose tissue (AT) of mice treated with tesa, (2), (3) or vehicle. Controls represent untreated mice and mice treated with vehicle (oral or intraperitoneal) ($n = 15$). Scale bar = 100 μM . Mean epi and sc adipocyte diameters were analyzed using the AxioVision software release 4.8.

of the plasma concentration of ketone bodies and adiponectin, whereas [F⁷, P³⁴]-NPY (2) and vehicle/untreated showed no effect (Figure 8C/E). Treatment had no major influence on the insulin and Mcp-1 levels (Figure 8D/G). The serum leptin concentration was reduced in the mice treated with tesa, whereas no reduction was detectable in all of the other treated mice (Figure 8F). Only tesaglitazar significantly enhanced the expression of PPAR γ in the liver (Figure 8H). The influence of tesa, tesa-NPY (3), and [F⁷, P³⁴]-NPY (2) on the plasma lipids was also analyzed (Figure 9). The vehicle/untreated *db/db* mice showed elevated levels of triglycerides and free fatty acids (FFA) compared to the lean C57BL/6N mice. Treatment with tesa and tesa-NPY (3) led to a normalization of the triglycerides, FFA, whereas [F⁷, P³⁴]-NPY (2) and vehicle/untreated had no influence on the lipid metabolism (Figure 9A/B). The cholesterol levels were unchanged by any treatment as these levels were also comparable in the untreated *db/db* mice compared to the lean mice (Figure 9C).

3.7. Microarray data analyses demonstrates differential expression of genes highly relevant to glucose metabolism and adipogenesis

To identify the regulated novel genes and pathways, we measured the mRNA expression in the adipose tissue of the treated and control mice using a microarray approach. In line with morphological changes observed in adipose tissue and metabolism under tesa-NPY, microarray data analyses revealed differential increases and decreases of genes highly relevant to glucose metabolism and adipogenesis (Table S1, S2, Figure 10). The gene expression comparison of the animals treated with tesa-NPY compared to [F⁷, P³⁴]-NPY identified ras homolog family

member B (*RhoB*) (logFC = -1.23, p-value = 0.00033), lens intrinsic membrane protein 2 (*Lims2*) (logFC = -0.87, p = 0.000209), fibroblast growth factor receptor-like 1 (*Fgfr1*) (log2FC = -0.9, p-value = 0.000820), C-X-C motif chemokine ligand 13 (*Cxcl13*) (logFC = 3.008, p-value = 0.00057), and the genes involved in antigen recognition s.a. *Ighv2-6-8* and *Ighv2-9-1* (Table S1 and S2) as highly regulated genes (Figure 10). The most significant enriched pathway of differentially expressed genes was related to lipid metabolism (fatty acid degradation and increased arachidonic and linoleic acid metabolism), the PPAR signaling pathway, drug metabolism in tesa-NPY treatment compared with FP-NPY, and insulin signaling (Table S3). Depleted pathways under tesa-NPY included cell cycle, cell turnover, apoptosis, and oxidative phosphorylation. Interestingly, the KEGG pathway for insulin signaling was downregulated although the gene ontology analyses of the biological processes and cell components showed enrichment of the gene sets involved in the positive regulation of glucose import and the negative regulation of the sequestering of triglycerides (Table S3).

4. DISCUSSION

Because of its beneficial effects on glucose and lipid abnormalities in patients with type 2 diabetes, PPAR α/γ agonist tesaglitazar is a promising candidate for clinical applications. However, severe side effects related to the essential role of PPAR in the regulation of numerous processes in a variety of cell types and tissues limit its therapeutic value. In this report, we describe the development of a system for the cell type-specific delivery of dual PPAR α/γ agonist tesa

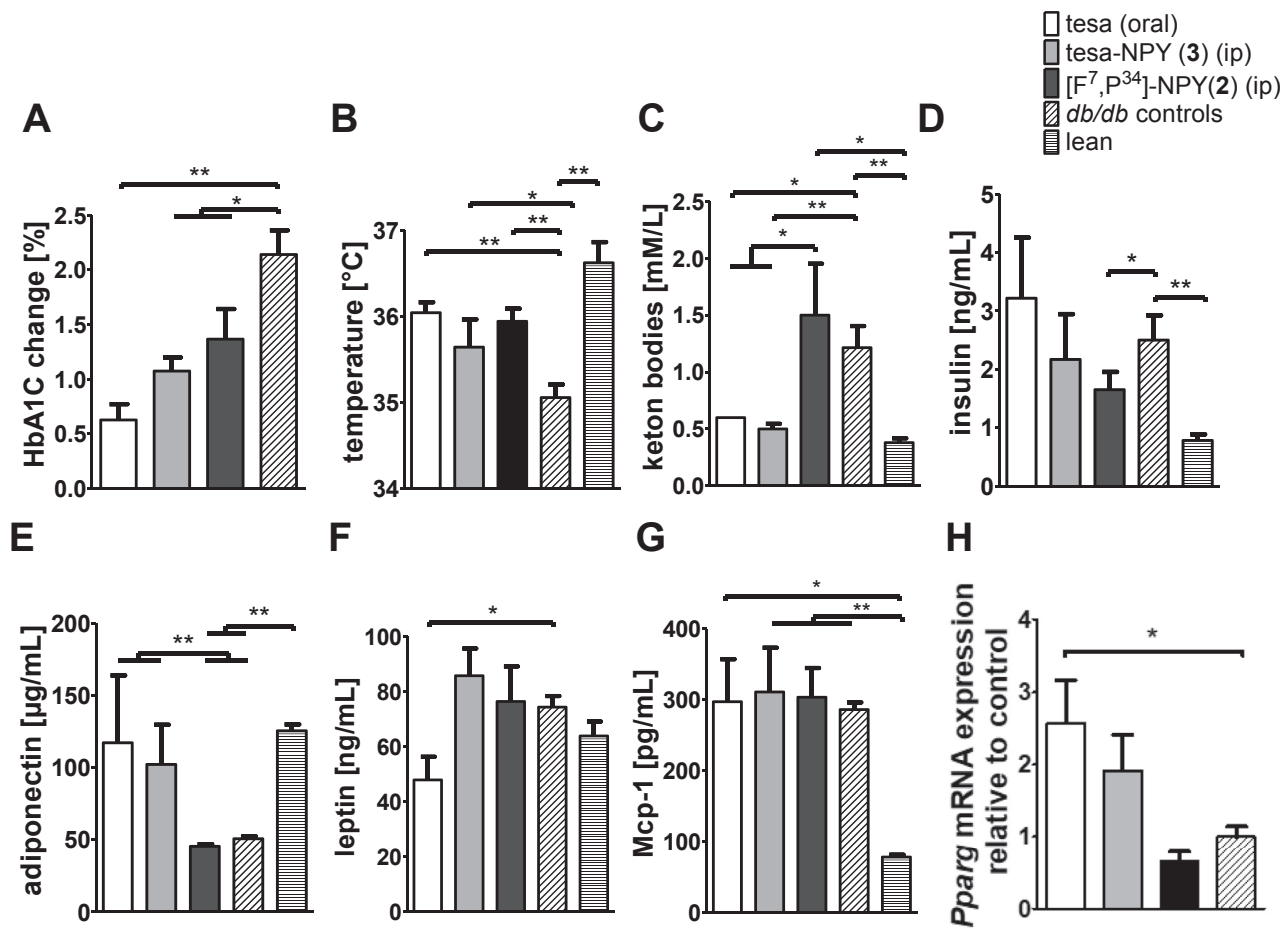


Figure 8: Influence of tesa-NPY (3) on metabolic parameters in *db/db* mice. (A–H) 2.5 µM/kg/day tesa, [F⁷, P³⁴]-NPY (2), or tesa-NPY (3) was administered for 8 days in *db/db* mice (n = 5) and different metabolic parameters including serum HbA1C change(A), temperature (B), ketone bodies (C), serum insulin (D), serum adiponectin (E), serum leptin (F), and serum Mcp-1 (G) were analyzed. In addition, PPARγ mRNA expression in liver was quantified relative to control animals (H). Controls represent untreated mice and mice treated with vehicle (oral or intraperitoneal) (n = 15). Values represented as mean ± SEM; *p ≤ 0.05, **p ≤ 0.01, ***p ≤ 0.001, according to the non-parametric Mann–Whitney U test.

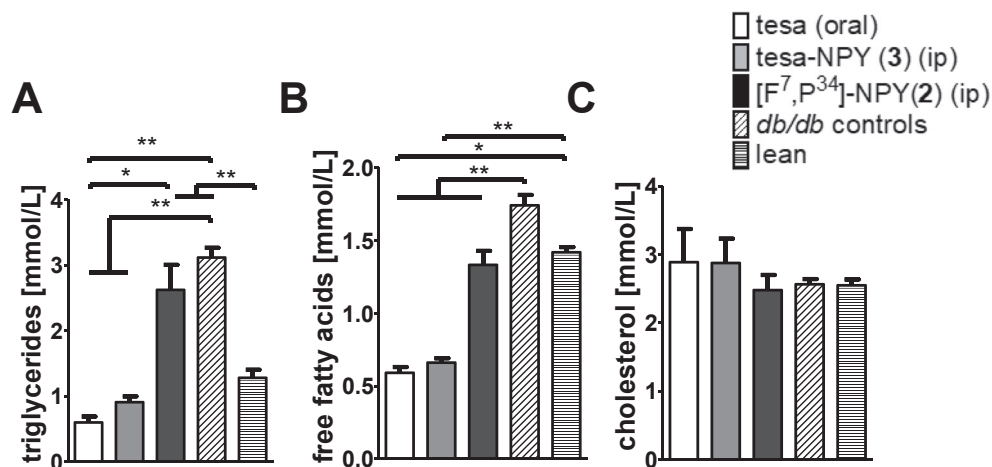


Figure 9: Influence of tesa-NPY (3) on plasma lipids in *db/db* mice. (A–C) 2.5 µM/kg/day tesa, [F⁷, P³⁴]-NPY (2), or tesa-NPY (3) was administered for 8 days in *db/db* mice (n = 5) and triglycerides (A), free fatty acids (B), and cholesterol (C) were analyzed. Controls represent untreated mice and mice treated with vehicle (oral or intraperitoneal) (n = 15). Values represent mean ± SEM; *p ≤ 0.05, **p ≤ 0.01, ***p ≤ 0.001, according to the non-parametric Mann–Whitney U test.

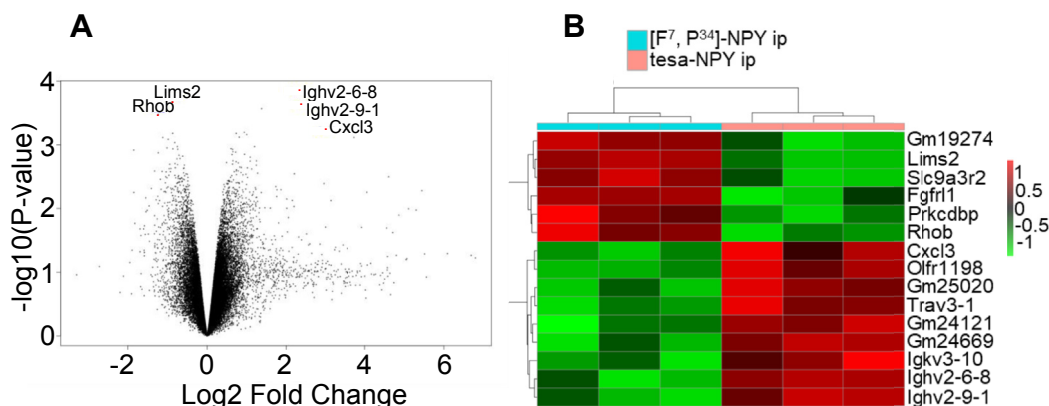


Figure 10: Microarray data analyses revealed differentially expressed genes between animals treated with tesa-NPY and [F7, P34]-NPY. (A) Volcano of differentially expressed genes in Tesa_NPY- vs FP_NPY-treated animals. RhoB ($p = 0.00033$), Lims2 ($p = 0.000209$), Fgfr1 (0.000820), and Cxcl3 ($p = 0.00057$) are highly regulated genes. Transcriptome profiling was performed in epigonodal samples of 3 mice from each experimental group using mouse Clariom™ S Assay from Affymetrix. Raw intensities values were background corrected, log₂ transformed and then quantile normalised. Log₂-transformed values were analyzed using the Bayesian moderated t-statistic. The linear model was fit to a design matrix including treatment as a factor variable with 2 levels and a “toptable” was produced with information on fold change in gene expression according to treatment, corresponding p-values and multiple testing adjusted p-values according to Benjamini Hochberg. (B) Heatmap with differentially regulated genes in Tesa_NPY- vs FP_NPY-treated animals with p -value < 0.001 .

into adipocytes. This strategy allows the use of PPAR α/γ agonists to selectively drive adipocyte differentiation and avoid their adverse effects in other tissues that has hindered the clinical development of these compounds. Peptide-drug conjugates, prodrugs synthesized by covalent coupling of a peptide to a drug via a specific cleavable linker, enter the cells by specific receptor-mediated binding and internalization in the receptor-expressing cells. Subsequent endosomal cleavage of the linker releases the drug to freely diffuse in the cells and exert its effects. Peptide-drug conjugates were investigated as a promising approach for the selective delivery of cytotoxic agents to tumors in cancer therapy and the first compounds are currently being evaluated in clinical trials [75]. Initial attempts to use this principle for the treatment of T2D have been achieved by targeting estrogen to GLP-1R-expressing tissues such as the pancreas [76].

4.1. Design of drug-peptide conjugates

We utilized NPY₁R as the cell surface receptor to selectively target adipocytes, as this GPCR was shown to be highly expressed in adipocytes and overexpressed in the adipose tissue of obese patients [27–30]. NPY₁R belongs to a multi-receptor multi-ligand family consisting of four receptor subtypes in humans (NPY₁R, NPY₂R, NPY₄R, and NPY₅R) that can be activated by NPY. Therefore, NPY₁R subtype selectivity of the carrier peptide is of high importance and has to be ensured [77,78]. This can be achieved by using [F⁷, P³⁴]-NPY, a NPY₁R-preferring peptide ligand, which was already successfully used to target NPY₁R-positive breast cancer cells [61–63,66,79,80]. We synthesized tesa-NPY (3), a conjugate consisting of PPAR α/γ agonist tesa attached to [F⁷, P³⁴]-NPY through a cleavable GFLG linker introduced at position K⁴. Tesa-NPY activates high-activity NPY₁R and robustly induces an internalization of the receptor. Furthermore, the investigation of the peptide conjugate among other human Y receptors demonstrated that tesa-NPY has very low activity at NPY₂R and NPY₄R. Interestingly, the modifications in the peptide conjugate led to a further reduction in activity at NPY₂R and NPY₄R compared to unmodified [F⁷, P³⁴]-NPY. This might be crucial especially with respect to NPY₄R, as this receptor is highly expressed in the gastrointestinal tract, pancreas, and prostate [81,82]. Selectivity toward cells expressing NPY₅R can also be ensured, as these receptors showed only minor internalization

and were mainly expressed in the CNS; thus, the effects at this receptor will be limited by the blood–brain barrier [34–36,80,83].

4.2. Successful specific peptide-mediated shuttling of tesa to NPY₁R-expressing cells

To prove NPY₁R-mediated PPAR γ activation by tesa-NPY, a PPAR γ reporter gene assay in NPY₁R-expressing HEK293 cells was performed. These assays demonstrated that tesa-NPY activated PPAR γ , proving that it was successfully internalized and released. The specific receptor-mediated internalization of the peptide conjugate was confirmed by testing cells lacking NPY₁R and by competition experiments using an excess of unlabeled NPY. Furthermore, cells that do not express PPAR γ did not respond to tesa-NPY. Thus, the potency of the conjugate is focused on cells expressing NPY₁R, enhancing PPAR γ and possibly also PPAR α activities, which we did not assess in our cell culture experiments. PPAR α also expressed in the adipose tissue has been shown to attenuate adiposity by promoting adipocyte differentiation and suppressing adipocyte hypertrophy [45]. Therefore, its additional activation by tesaglitazar shuttled to adipocytes would additionally enhance the beneficial effects. In addition to adipocytes, neurons and vascular smooth muscle cells are the only known other cell types that express both NPY₁R and PPAR γ and thus might also be targeted by the peptide conjugate. The transport of PPAR γ agonists to the CNS is hindered by the low NPY peptide permeability of the blood–brain barrier [34–36]. However, it can be expected that uptake might also occur in the vascular smooth muscle cells. The activation of PPAR γ in vascular smooth muscle cells resulted in improved inflammation, coronary insulin resistance, and upregulation of adiponectin receptor expression and might even improve the health of patients with T2D [84,85]. In addition to the co-expression of NPY₁R and PPAR α in the adipocytes, both proteins are mainly co-expressed in the kidney (<https://www.proteinatlas.org>). The Y1 receptor is primarily a renal vascular receptor [86], and PPAR α acts as an antiatherogenic factor by modulating local and systemic inflammatory responses. PPAR α ligands have beneficial effects on diabetic nephropathy and have been shown to be protective in chronic kidney diseases [87]. Thus, targeting of vascular smooth muscle cells in addition to adipocytes should not lead to side effects.

4.3. Tesa-NPY enhances adipogenesis and is a suitable candidate for in vivo studies

After the initial proof of concept studies, further investigations revealed that tesa-NPY enhanced adipogenesis in murine 3T3-L1 cells, demonstrating that it was successfully internalized and released in cells natively expressing NPY₁R. To strengthen this finding, we examined the expression of the PPAR γ -responsive genes adiponectin, Fabp4, and Cidec [71–74,88–91]. Adiponectin may mediate the beneficial effects of PPAR γ agonists for the treatment of diabetes, as it is an insulin-sensitizing adipokine that affects hepatic glucose output and decreases triglyceride content in the liver and muscle [92]. Cha et al. showed that tesa induces increased adiponectin mRNA expression and plasma levels in *db/db* mice, which improves insulin resistance [93]. Fapb4 is needed to transport fatty acids through the cytoplasm, and Cidec is involved in lipid droplet formation, so both regulate lipid metabolism and are thus highly expressed in mature adipocytes [72,88]. Tesa and tesa-NPY enhanced the expression of adiponectin and shifted it to earlier time points in the differentiation procedure. Fapb4 and Cidec were only significantly induced by tesa treatment at the time points studied. Because the peptides were added simultaneously with highly optimized differentiation medium, the effect of treatment with tesa or peptides was overlaid by additional enhancing factors. This was reflected by a very strong increase in the adiponectin, Fapb4, and Cidec expression between days 3 and 4 even in the control DMSO treatment (for example, > 100 fold for adiponectin on day 4/day 3 and even higher for the other genes; data not shown). Furthermore, it was also underlined by the shift in the observed effects to earlier time points, which especially for tesa-NPY were hardly detectable on day 4 as opposed to day 3. The effects were easier to detect for tesa taken up by passive diffusion in substantial amounts than tesa-NPY, which was dependent on the receptor internalization. This was observed in the previously discussed PPAR reporter assays. To obtain more significant results, it would be necessary to optimize the relationship of the peptide treatment duration, enhancing the effect and minimizing the side effects in the differentiation protocol, already optimized to reach high differentiation rates in vitro. Nevertheless, significant results were obtained for 3T3 differentiation and the induction of adiponectin expression on day 3 and a similar trend was also observed in the SGBS cells, although it did not reach significant differences for tesa-NPY. These results illustrate that tesa-NPY can induce established PPAR γ effects, such as induction of adipogenesis and adiponectin expression, which are beneficial for the treatment of diabetes as they lead to insulin sensitization. Thus, tesa-NPY possessed optimal requirements for in vivo studies.

4.4. In vivo studies demonstrate the anti-diabetic activity of the peptide-drug conjugate

Previous in vivo studies demonstrated that free systemically administered tesa can reduce hypertriglyceridemia, hyperinsulinemia, and hyperglycemia in *ob/ob* mice and restore insulin sensitivity in obese Zucker rats [43]. It also reduces atherosclerosis in LDL receptor-deficient mice [94]. In the present study, we used *db/db* mice to evaluate the anti-diabetic potency of the peptide conjugate, as these mice are known to develop severe insulin resistance and hypertriglyceridemia [95,96]. Phenotypical characterization revealed that the animals that did not receive tesa or tesa-NPY lost 3% of their body weight during the treatment period. During this time, all of the mice were 12–16 weeks old; *db/db* mice are known to suffer from severe disease syndromes such as progressive hyperglycemia and glucosuria, which lead to the loss of calories and thus body weight [97–99]. Treatment with tesa and tesa-NPY can prevent this weight loss, indicating a prevention of calorie loss through glucosuria by improved

glycemic control as previously shown for other PPAR γ agonists in diabetic ZDF rats [97,100]. Ljung et al. showed that tesa treatment does not lead to weight gain in treated animals, which is usually seen in traditional PPAR γ agonists such as rosiglitazone [74]. In the present study, no body weight gain was detected and no major differences between the treated and untreated animals regarding body composition could be measured, as all of the groups lost fat and gained lean mass.

In contradiction to previous tesa in vivo studies, no major improvements in hyperglycemia (serum HbA1C) and serum insulin levels were detected in the treated mice compared to the untreated animals [43]. However, treatment with tesa or tesa-NPY did result in a deceleration of disease progression, which is characterized by increasing blood glucose values that could have been prevented by tesa and tesa-NPY in the present study. No major changes in the total serum glucose occurred and the insulin levels remained unchanged as the mice adapted to the amount of glucose in their blood. An additional reason for the constant insulin values might be the age of the animals, which was not comparable between the study of Ljung et al. who used 6-week-old mice, and the present study, which utilized 12- to 16-week-old mice [43]. *Ob/ob* and *db/db* mice up to three months old are characterized by strongly elevated serum insulin levels that are supposed to compensate for rising blood sugar concentrations. Afterward, disease progression results in a decline in serum insulin and decreased levels due to the destruction of pancreatic islets and the loss of β -cells [98]. At this stage, the destruction of β -cells might be too advanced to be restored by tesa treatment for only one week. Longer treatment periods might lead to better control of the glucose and insulin levels, which was previously shown for the PPAR α/γ agonist muraglitazar in 12-week-old *db/db* mice, whereas treatment for one week did not lead to significant effects, whereas treatment for 2–4 weeks did [100].

Metabolomic studies of mice and humans have identified many plasma metabolite signatures in addition to HbA1C and insulin that are associated with the development and progression of T2D, such as high serum concentrations of FFAs, triglycerides, ketone bodies, leptin, and pro-inflammatory cytokines such as Mcp-1 and a low serum concentration of adiponectin [101–107]. All of these factors promote the manifestation of T2D. Increased concentrations of circulating FFAs, for example, are major factors eliciting systemic insulin resistance [108]. High plasma concentrations of FFAs, triglycerides, and ketone bodies and low levels of circulating adiponectin were normalized by tesa and tesa-NPY treatment, but no significant effect on leptin and Mcp-1 was detected. In summary, the tesa-NPY conjugate revealed promising anti-diabetic effects, as the present study demonstrated that it improved most of the aforementioned metabolic parameters and corrected hypertriglyceridemia.

As tesa-NPY, selectively transported to NPY₁R-expressing cells, performed as well as systemically administered tesa, adipocyte-specific PPAR γ activation is obviously sufficient for reversing metabolic parameters to a similar degree as systemic PPAR γ activation. This was demonstrated by Sugii et al. who used PPAR γ agonists to restore the whole body insulin resistance of HFD mice that expressed PPAR γ in an adipocyte-specific manner as efficiently as mice that expressed PPAR γ systemically [109]. Thus, the observed anti-diabetic effects are assumed to result from adipocyte-specific PPAR γ -mediated mechanisms. These include the release of insulin-sensitizing and anti-inflammatory adipokines such as adiponectin, and the lowering of plasma FFA and TG levels by uptake into newly differentiated adipocytes [9,110]. Both these effects were detected in the present study. Adipose tissue histology confirmed smaller adipocyte size and thus adipogenesis only in the mice treated with tesa-NPY. Tesaglitazar is an

orally active agent on a whole body level [43], whereas tesa-NPY acts selectively on NPY-expressing tissues such as adipose tissue and must be administered intraperitoneally. Both tesa and tesa-NPY improve the metabolic state but tesa-NPY selectively acts on adipose tissue. Studies of volunteers demonstrated that tesaglitazar is rapidly and completely absorbed after oral dosing and has linear pharmacokinetic properties, with an elimination half-life of between 38 and 59 h [111]. Therefore, only tesa-NPY can exert marked effects on adipose tissue. In agreement with this phenotype, the KEGG pathways showed increased fatty acid transport through *Fabp4*, although the LPL pathway was downregulated. Furthermore, perilipin decreased blunting access to the TGs and therefore reduced sequestration by active lipases. The fatty acid and beta oxidation pathways were significantly enriched. These mechanisms warrant the potential of tesa-NPY for metabolic disease improvement.

In line with the morphological changes in the adipose tissue and metabolism under tesa-NPY, the microarray data analyses demonstrated differential increases and decreases in the genes highly relevant to glucose metabolism and adipogenesis. The loss of *RhoB*, a downregulated gene in animals treated with tesa-NPY compared to $[F^7, P^{34}]$ -NPY, has been shown to prevent streptozotocin-induced diabetes and ameliorate diabetic complications in mice, which could indicate the positive effects of tesa-NPY in the absence of HbA1c differences between the delay in disease progression in animals under treatment [112]. *Lims2* was downregulated in tesa-NPY treatment. In the literature, *lims2* is described as interacting with *GP17*, whose deletion has been shown to increase body weight without changing food intake although *lims2* deficient mice do not demonstrate a specific obese phenotype [113]. The downregulation of *Lims2* under tesa-NPY can mediate the prevention of weight loss in diabetic animals compared to untreated animals. In addition, *FGFRL1* decreased under tesa-NPY. *FGFRL1* is the fifth member of the fibroblast growth factor receptor (*FGFR*). It interacts with fibroblast growth factors to induce differentiation and plays a key role during embryonic development [114]. This gene is highly expressed in subcutaneous and epigonadal fat pads in mice. The expression of *FGFRL1* and *FGFR1* increased during adipocyte differentiation from mesenchymal stromal cells, was more highly expressed in pre-adipocytes compared to adipocytes, and *FGFR1* knockdown further inhibited adipocyte differentiation [115]. However, mice treated with tesa-NPY demonstrated unregulated *CXCL13*, which has been shown to be highly expressed in mature adipocytes compared to pre-adipocytes and mediate B-cell uptake to the liver in *ob/ob* mice [116]. The interplay of these genes in adipogenesis and differentiation could demonstrate the essential role of tesa-NPY treatment in active adipocyte differentiation and maturation, supporting data from the AT histology and cell culture studies presented.

The mice treated with free tesa showed a trend toward smaller adipocyte size and also demonstrated a reduction in plasma FFAs and TGs. This was because the insulin-sensitizing effects of PPAR γ agonists do not depend only on adipogenesis. Sugii et al. showed that PPAR γ activation in mature adipocytes but not preadipocytes (and hence no activation of adipogenesis) was sufficient to improve insulin sensitivity [109]. Thus, lower plasma FFA and TG levels can be explained by the second PPAR γ -mediated mechanism, which is the release of adipokines such as adiponectin. Adiponectin is known to enhance FFA uptake and oxidation in the muscle and liver, leading to decreased circulating FFAs [92,117]. The reduction in plasma FFAs then correlates with a mobilization of lipids out of the liver and muscle, thus improving whole body insulin sensitivity [110,118].

Impaired thermoregulation is another well-documented characteristic of diabetic mice. At temperatures of approximately 30 °C, which were used in the present study, the body temperature of *db/db* mice was approximately 1 °C lower than that of lean C57BL/6N mice [119,120]. The body temperature could be normalized by treatment with tesa, tesa-NPY, and $[F^7, P^{34}]$ -NPY, proving that not only tesa but also $[F^7, P^{34}]$ -NPY can have beneficial effects. This is in accordance with the literature, as the body temperature of mice increases if they are administered NPY in the paraventricular nucleus, yet no investigation in mice has been performed to date demonstrating the same effect for NPY administered peripherally [121]. Moreover, in endotoxemic rats, a single dose of peripherally injected NPY stabilized their body temperature [122].

In contrast to adipose tissue, there is very low expression of PPAR γ and even less NPY $_1$ R in human and mouse livers (<http://www.informatics.jax.org/expression.shtml>; <https://www.proteinatlas.org>). We found that tesaglitazar significantly enhanced the expression of PPAR γ in the liver. Tesa is a dual agonist of PPAR α and γ that improves both lipidemic and glycemic abnormalities in preclinical models of type 2 diabetes and metabolic syndrome [43, 123,124]. The tesa-NPY conjugate also elevates PPAR γ expression but not significantly. That elevation might be due to the fatty liver in *db/db* mice. *Db/db* mice exhibit non-alcoholic fatty liver disease (NAFLD) with adipocytes. Further investigations will be required to determine whether isolated hepatocytes represent stable noninfluenced PPAR γ expression in non-fatty tissues.

5. CONCLUSION

In conclusion, we developed a novel system for the cell-type specific uptake of a PPAR α/γ dual agonists by peptide-mediated internalization and controlled release into adipocytes. Treatment of adipocytes with peptide conjugate enhanced adipogenesis and adiponectin expression. In vivo studies using *db/db* mice proved the ability of the peptide conjugate to prevent diabetes progression by reducing plasma FFAs and hypertriglyceridemia and enhancing plasma adiponectin levels as efficient as systemically administered tesa. These data clearly demonstrated that a peptide conjugate composed of $[F^7, P^{34}]$ -NPY and tesa is as efficient as free tesa and is thus a promising drug candidate that potentially reduces the known side effects of non-selective PPAR γ agonists for the treatment of T2D.

AUTHOR CONTRIBUTIONS

SW and AB-S conceived the study, designed and conducted the experiments, analyzed the data, and wrote the paper. NK conducted the mouse experiments, contributed to the discussion, and reviewed the manuscript. RC performed the microarray data analyses, wrote respective sections, contributed to the discussion, and reviewed the manuscript. KM and MB reviewed the manuscript. All the authors discussed the results and commented on the manuscript. AB-S supervised the project.

ACKNOWLEDGMENTS

Kristin Löbner, Regina Reppich-Sacher, Ronny Müller, Jenny Schuster, and Daniela Kern are acknowledged for their technical assistance during the cell culture, solid phase peptide synthesis, and in vivo studies. We also thank the Integrated Research and Treatment Center (IFB) AdipositasErkrankungen, Fonds der Chemischen Industrie, the German Science Foundation Project number 209933838 – SFB 1052, 1052/A3, B1, B4, and the European Union for generous funding.

CONFLICTS OF INTEREST

No potential conflicts of interest relevant to this article were reported.

APPENDIX A. SUPPLEMENTARY DATA

Supplementary data to this article can be found online at <https://doi.org/10.1016/j.molmet.2019.11.009>.

REFERENCES

- [1] Seidell, J.C., 2000. Obesity, insulin resistance and diabetes—a worldwide epidemic. *British Journal of Nutrition* 83(Suppl 1):S5–S8.
- [2] Field, A.E., Coakley, E.H., Must, A., Spadano, J.L., Laird, N., Dietz, W.H., et al., 2001. Impact of overweight on the risk of developing common chronic diseases during a 10-year period. *Archives of Internal Medicine* 161(13):1581–1586.
- [3] Must, A., Spadano, J., Coakley, E.H., Field, A.E., Colditz, G., Dietz, W.H., 1999. The disease burden associated with overweight and obesity. *Journal of the American Medical Association* 282(16):1523–1529.
- [4] Kloting, N., Bluher, M., 2014. Adipocyte dysfunction, inflammation and metabolic syndrome. *Reviews in Endocrine & Metabolic Disorders* 15(4):277–287.
- [5] Bjorntorp, P., Sjöström, L., 1971. Number and size of adipose tissue fat cells in relation to metabolism in human obesity. *Metabolism Clinical and Experimental* 20(7):703–713.
- [6] Weyer, C., Foley, J.E., Bogardus, C., Tataranni, P.A., Pratley, R.E., 2000. Enlarged subcutaneous abdominal adipocyte size, but not obesity itself, predicts type II diabetes independent of insulin resistance. *Diabetologia* 43(12):1498–1506.
- [7] Spalding, K.L., Arner, E., Westermark, P.O., Bernard, S., Buchholz, B.A., Bergmann, O., et al., 2008. Dynamics of fat cell turnover in humans. *Nature* 453(7196):783–787.
- [8] Ahmadian, M., Suh, J.M., Hah, N., Liddle, C., Atkins, A.R., Downes, M., et al., 2013. PPARγ signaling and metabolism: the good, the bad and the future. *Nature Medicine* 19(5):557–566.
- [9] Berger, J., Moller, D.E., 2002. The mechanisms of action of PPARs. *Annual Review of Medicine* 53:409–435.
- [10] Guo, L., Tabrizchi, R., 2006. Peroxisome proliferator-activated receptor gamma as a drug target in the pathogenesis of insulin resistance. *Pharmacology & Therapeutics* 111(1):145–173.
- [11] Lehmann, J.M., Moore, L.B., Smith-Oliver, T.A., Wilkison, W.O., Willson, T.M., Kliewer, S.A., 1995. An antidiabetic thiazolidinedione is a high affinity ligand for peroxisome proliferator-activated receptor gamma (PPAR gamma). *Journal of Biological Chemistry* 270(22):12953–12956.
- [12] Yamauchi, T., Kamon, J., Waki, H., Murakami, K., Motojima, K., Komeda, K., et al., 2001. The mechanisms by which both heterozygous peroxisome proliferator-activated receptor gamma (PPARγ) deficiency and PPARγ agonist improve insulin resistance. *Journal of Biological Chemistry* 276(44):41245–41254.
- [13] Kim, J.K., Fillmore, J.J., Gavrilova, O., Chao, L., Higashimori, T., Choi, H., et al., 2003. Differential effects of rosiglitazone on skeletal muscle and liver insulin resistance in A-ZIP/F-1 fatless mice. *Diabetes* 52(6):1311–1318.
- [14] Salomone, S., 2011. Pleiotropic effects of glitazones: a double edge sword? *Frontiers in Pharmacology* 2:14.
- [15] Azoulay, L., Yin, H., Filion, K.B., Assayag, J., Majdan, A., Pollak, M.N., et al., 2012. The use of pioglitazone and the risk of bladder cancer in people with type 2 diabetes: nested case-control study. *BMJ* 344:e3645.
- [16] Balakumar, P., Rose, M., Ganti, S.S., Krishan, P., Singh, M., 2007. PPAR dual agonists: are they opening Pandora's Box? *Pharmacological Research* 56(2): 91–98.
- [17] Graham, D.J., Ouellet-Hellstrom, R., MaCurdy, T.E., Ali, F., Sholley, C., Worrall, C., et al., 2010. Risk of acute myocardial infarction, stroke, heart failure, and death in elderly Medicare patients treated with rosiglitazone or pioglitazone. *Journal of the American Medical Association* 304(4):411–418.
- [18] Kung, J., Henry, R.R., 2012. Thiazolidinedione safety. *Expert Opinion on Drug Safety* 11(4):565–579.
- [19] Nissen, S.E., Wolski, K., 2007. Effect of rosiglitazone on the risk of myocardial infarction and death from cardiovascular causes. *New England Journal of Medicine* 356(24):2457–2471.
- [20] Burant, C.F., Sreenan, S., Hirano, K., Tai, T.A., Lohmiller, J., Lukens, J., et al., 1997. Troglitazone action is independent of adipose tissue. *Journal of Clinical Investigation* 100(11):2900–2908.
- [21] Ahrens, V.M., Bellmann-Sickert, K., Beck-Sickinger, A.G., 2012. Peptides and peptide conjugates: therapeutics on the upward path. *Future Medicinal Chemistry* 4(12):1567–1586.
- [22] Made, V., Els-Heindl, S., Beck-Sickinger, A.G., 2014. Automated solid-phase peptide synthesis to obtain therapeutic peptides. *Beilstein Journal of Organic Chemistry* 10:1197–1212.
- [23] Reubi, J.C., 2003. Peptide receptors as molecular targets for cancer diagnosis and therapy. *Endocrine Reviews* 24(4):389–427.
- [24] Bohme, D., Beck-Sickinger, A.G., 2015. Drug delivery and release systems for targeted tumor therapy. *Journal of Peptide Science — An Official Publication of the European Peptide Society* 21(3):186–200.
- [25] Majumdar, S., Siahaan, T.J., 2012. Peptide-mediated targeted drug delivery. *Medicinal Research Reviews* 32(3):637–658.
- [26] Ferguson, S.S., 2001. Evolving concepts in G protein-coupled receptor endocytosis: the role in receptor desensitization and signaling. *Pharmacological Reviews* 53(1):1–24.
- [27] Amisten, S., Neville, M., Hawkes, R., Persaud, S.J., Karpe, F., Salehi, A., 2015. An atlas of G-protein coupled receptor expression and function in human subcutaneous adipose tissue. *Pharmacology & Therapeutics* 146:61–93.
- [28] Gericke, M.T., Kosacka, J., Koch, D., Nowicki, M., Schroder, T., Ricken, A.M., et al., 2009. Receptors for NPY and PACAP differ in expression and activity during adipogenesis in the murine 3T3-L1 fibroblast cell line. *British Journal of Pharmacology* 157(4):620–632.
- [29] Serradeil-Le Gal, C., Lafontan, M., Raufaste, D., Marchand, J., Pouzet, B., Casellas, P., et al., 2000. Characterization of NPY receptors controlling lipolysis and leptin secretion in human adipocytes. *FEBS Letters* 475(2):150–156.
- [30] Sitticharoon, C., Chatree, S., Churintaraphan, M., 2013. Expressions of neuropeptide Y and Y1 receptor in subcutaneous and visceral fat tissues in normal weight and obese humans and their correlations with clinical parameters and peripheral metabolic factors. *Regulatory Peptides* 185: 65–72.
- [31] Eva, C., Keinanen, K., Monyer, H., Seeburg, P., Sprengel, R., 1990. Molecular cloning of a novel G protein-coupled receptor that may belong to the neuropeptide receptor family. *FEBS Letters* 271(1–2):81–84.
- [32] Inui, A., 1999. Neuropeptide Y feeding receptors: are multiple subtypes involved? *Trends in Pharmacological Sciences* 20(2):43–46.
- [33] Uddman, R., Moller, S., Nilsson, T., Nystrom, S., Ekstrand, J., Edvinsson, L., 2002. Neuropeptide Y Y1 and neuropeptide Y Y2 receptors in human cardiovascular tissues. *Peptides* 23(5):927–934.
- [34] Kastin, A.J., Akerstrom, V., 1999. Nonsaturable entry of neuropeptide Y into brain. *American Journal of Physiology* 276(3 Pt 1):E479–E482.
- [35] Krysiak, R., Obuchowicz, E., Herman, Z.S., 1999. Interactions between the neuropeptide Y system and the hypothalamic-pituitary-adrenal axis. *European Journal of Endocrinology* 140(2):130–136.
- [36] Zhang, W., Cline, M.A., Gilbert, E.R., 2014. Hypothalamus-adipose tissue crosstalk: neuropeptide Y and the regulation of energy metabolism. *Nutrition & Metabolism* 11:27.
- [37] Kuo, L.E., Kitlinska, J.B., Tilan, J.U., Li, L., Baker, S.B., Johnson, M.D., et al., 2007. Neuropeptide Y acts directly in the periphery on fat tissue and mediates stress-induced obesity and metabolic syndrome. *Nature Medicine* 13(7):803–811.

- [38] Yang, K., Guan, H., Arany, E., Hill, D.J., Cao, X., 2008. Neuropeptide Y is produced in visceral adipose tissue and promotes proliferation of adipocyte precursor cells via the Y1 receptor. *The FASEB Journal — Official Publication of the Federation of American Societies for Experimental Biology* 22(7): 2452–2464.
- [39] Tang, H.N., Man, X.F., Liu, Y.Q., Guo, Y., Tang, A.G., Liao, E.Y., et al., 2015. Dose-dependent effects of neuropeptide Y on the regulation of preadipocyte proliferation and adipocyte lipid synthesis via the PPARgamma pathways. *Endocrine Journal* 62(9):835–846.
- [40] Cariou, B., Charbonnel, B., Staels, B., 2012. Thiazolidinediones and PPAR-gamma agonists: time for a reassessment. *Trends in Endocrinology and Metabolism— TEM* 23(5):205–215.
- [41] Bays, H., McElhattan, J., Bryzinski, B.S., 2007. A double-blind, randomised trial of tesaglitazar versus pioglitazone in patients with type 2 diabetes mellitus. *Diabetes and Vascular Disease Research* 4(3):181–193.
- [42] Goldstein, B.J., Rosenstock, J., Anzalone, D., Tou, C., Ohman, K.P., 2006. Effect of tesaglitazar, a dual PPAR alpha/gamma agonist, on glucose and lipid abnormalities in patients with type 2 diabetes: a 12-week dose-ranging trial. *Current Medical Research and Opinion* 22(12):2575–2590.
- [43] Ljung, B., Bamberg, K., Dahlof, B., Kjellstedt, A., Oakes, N.D., Ostling, J., et al., 2002. AZ 242, a novel PPARalpha/gamma agonist with beneficial effects on insulin resistance and carbohydrate and lipid metabolism in ob/ob mice and obese Zucker rats. *The Journal of Lipid Research* 43(11):1855–1863.
- [44] Conolon, D., 2006. Goodbye glitazars? *The British Journal of Diabetes & Vascular Disease* 6:135–137.
- [45] Goto, T., Lee, J.Y., Teraminami, A., Kim, Y.I., Hirai, S., Uemura, T., et al., 2011. Activation of peroxisome proliferator-activated receptor-alpha stimulates both differentiation and fatty acid oxidation in adipocytes. *The Journal of Lipid Research* 52(5):873–884.
- [46] Tsuchida, A., Yamauchi, T., Takekawa, S., Hada, Y., Ito, Y., Maki, T., et al., 2005. Peroxisome proliferator-activated receptor (PPAR)alpha activation increases adiponectin receptors and reduces obesity-related inflammation in adipose tissue: comparison of activation of PPARalpha, PPARgamma, and their combination. *Diabetes* 54(12):3358–3370.
- [47] Grundy, S.M., Benjamin, I.J., Burke, G.L., Chait, A., Eckel, R.H., Howard, B.V., et al., 1999. Diabetes and cardiovascular disease: a statement for healthcare professionals from the American Heart Association. *Circulation* 100(10): 1134–1146.
- [48] Tenenbaum, A., Motro, M., Fisman, E.Z., 2005. Dual and pan-peroxisome proliferator-activated receptors (PPAR) co-agonism: the bezafibrate lessons. *Cardiovascular Diabetology* 4:14.
- [49] Schubert, M., Stichel, J., Du, Y., Tough, I.R., Sliwoski, G., Meiler, J., et al., 2017. Identification and characterization of the first selective Y4 receptor positive allosteric modulator. *Journal of Medicinal Chemistry* 60(17):7605–7612.
- [50] Bohme, D., Kriehoff, J., Beck-Sickinger, A.G., 2016. Double methotrexate-modified neuropeptide Y analogues express increased toxicity and overcome drug resistance in breast cancer cells. *Journal of Medicinal Chemistry* 59(7):3409–3417.
- [51] Wabitsch, M., Brenner, R.E., Melzner, I., Braun, M., Moller, P., Heinze, E., et al., 2001. Characterization of a human preadipocyte cell strain with high capacity for adipose differentiation. *International Journal of Obesity and Related Metabolic Disorders — Journal of the International Association for the Study of Obesity* 25(1):8–15.
- [52] Krowczynska, A.M., Coutts, M., Makrides, S., Brawerman, G., 1989. The mouse homologue of the human acidic ribosomal phosphoprotein PO: a highly conserved polypeptide that is under translational control. *Nucleic Acids Research* 17(15):6408.
- [53] Kloting, N., Koch, L., Wunderlich, T., Kern, M., Ruschke, K., Krone, W., et al., 2008. Autocrine IGF-1 action in adipocytes controls systemic IGF-1 concentrations and growth. *Diabetes* 57(8):2074–2082.
- [54] Berry, R., Church, C.D., Gericke, M.T., Jeffery, E., Colman, L., Rodeheffer, M.S., 2014. Imaging of adipose tissue. *Methods in Enzymology* 537:47–73.
- [55] Irizarry, R.A., Hobbs, B., Collin, F., Beazer-Barclay, Y.D., Antonellis, K.J., Scherf, U., et al., 2003. Exploration, normalization, and summaries of high density oligonucleotide array probe level data. *Biostatistics* 4(2):249–264.
- [56] Ritchie, M.E., Phipson, B., Wu, D., Hu, Y., Law, C.W., Shi, W., et al., 2015. Limma powers differential expression analyses for RNA-sequencing and microarray studies. *Nucleic Acids Research* 43(7):e47.
- [57] Eden, E., Navon, R., Steinfeld, I., Lipson, D., Yakhini, Z., 2009. GOrilla: a tool for discovery and visualization of enriched GO terms in ranked gene lists. *BMC Bioinformatics* 10:48.
- [58] Luo, W., Brouwer, C., 2013. Pathview: an R/Bioconductor package for pathway-based data integration and visualization. *Bioinformatics* 29(14):1830–1831.
- [59] Wickham, H., 2009. *ggplot2: elegant graphics for data analysis*. New York: New York: Springer-Verlag.
- [60] Supek, F., Bosnjak, M., Skunca, N., Smuc, T., 2011. REVIGO summarizes and visualizes long lists of gene ontology terms. *PLoS One* 6(7):e21800.
- [61] Soll, R.M., Dinger, M.C., Lundell, I., Larhammer, D., Beck-Sickinger, A.G., 2001. Novel analogues of neuropeptide Y with a preference for the Y1-receptor. *European Journal of Biochemistry* 268(10):2828–2837.
- [62] Ahrens, V.M., Frank, R., Stadlbauer, S., Beck-Sickinger, A.G., Hey-Hawkins, E., 2011. Incorporation of ortho-carboranyl-N-epsilon-modified L-lysine into neuropeptide Y receptor Y1- and Y2-selective analogues. *Journal of Medicinal Chemistry* 54(7):2368–2377.
- [63] Ahrens, V.M., Kostelnik, K.B., Rennert, R., Bohme, D., Kalkhof, S., Kosel, D., et al., 2015. A cleavable cytolysin-neuropeptide Y bioconjugate enables specific drug delivery and demonstrates intracellular mode of action. *Journal of Controlled Release — Official Journal of the Controlled Release Society* 209:170–178.
- [64] Zwanziger, D., Khan, I.U., Neundorf, I., Sieger, S., Lehmann, L., Friebe, M., et al., 2008. Novel chemically modified analogues of neuropeptide Y for tumor targeting. *Bioconjugate Chemistry* 19(7):1430–1438.
- [65] Neer, E.J., 1995. Heterotrimeric G proteins: organizers of transmembrane signals. *Cell* 80(2):249–257.
- [66] Bohme, D., Beck-Sickinger, A.G., 2015. Controlling toxicity of Peptide-drug conjugates by different chemical linker structures. *ChemMedChem* 10(5): 804–814.
- [67] Made, V., Babilon, S., Jolly, N., Wanka, L., Bellmann-Sickert, K., Diaz Gimenez, L.E., et al., 2014. Peptide modifications differentially alter G protein-coupled receptor internalization and signaling bias. *Angewandte Chemie* 53(38):10067–10071.
- [68] Bohme, I., Stichel, J., Walther, C., Morl, K., Beck-Sickinger, A.G., 2008. Agonist induced receptor internalization of neuropeptide Y receptor subtypes depends on third intracellular loop and C-terminus. *Cellular Signalling* 20(10):1740–1749.
- [69] Tontonoz, P., Hu, E., Spiegelman, B.M., 1994. Stimulation of adipogenesis in fibroblasts by PPAR gamma 2, a lipid-activated transcription factor. *Cell* 79(7):1147–1156.
- [70] Greenberger, J.S., 1979. Corticosteroid-dependent differentiation of human marrow preadipocytes in vitro. *In Vitro* 15(10):823–828.
- [71] Choi, S.S., Kim, E.S., Koh, M., Lee, S.J., Lim, D., Yang, Y.R., et al., 2014. A novel non-agonist peroxisome proliferator-activated receptor gamma (PPARgamma) ligand UHC1 blocks PPARgamma phosphorylation by cyclin-dependent kinase 5 (CDK5) and improves insulin sensitivity. *Journal of Biological Chemistry* 289(38):26618–26629.
- [72] Cignarelli, A., Perrini, S., Nigro, P., Ficarella, R., Barbaro, M., Pescechera, A., et al., 2016. Long-acting insulin analog detemir displays reduced effects on adipocyte differentiation of human subcutaneous and visceral adipose stem cells. *Nutrition, Metabolism, and Cardiovascular Diseases — NMCD* 26(4):333–344.

- [73] Hwang, H.H., Moon, P.G., Lee, J.E., Kim, J.G., Lee, W., Ryu, S.H., et al., 2011. Identification of the target proteins of rosiglitazone in 3T3-L1 adipocytes through proteomic analysis of cytosolic and secreted proteins. *Molecules and Cells* 31(3):239–246.
- [74] Yang, W.S., Jeng, C.Y., Wu, T.J., Tanaka, S., Funahashi, T., Matsuzawa, Y., et al., 2002. Synthetic peroxisome proliferator-activated receptor-gamma agonist, rosiglitazone, increases plasma levels of adiponectin in type 2 diabetic patients. *Diabetes Care* 25(2):376–380.
- [75] Kaspar, A.A., Reichert, J.M., 2013. Future directions for peptide therapeutics development. *Drug Discovery Today* 18(17–18):807–817.
- [76] Finan, B., Yang, B., Ottaway, N., Stemmer, K., Muller, T.D., Yi, C.X., et al., 2012. Targeted estrogen delivery reverses the metabolic syndrome. *Nature Medicine* 18(12):1847–1856.
- [77] Michel, M.C., Beck-Sickinger, A., Cox, H., Doods, H.N., Herzog, H., Larhammar, D., et al., 1998. XVI. International Union of Pharmacology recommendations for the nomenclature of neuropeptide Y, peptide YY, and pancreatic polypeptide receptors. *Pharmacological Reviews* 50(1):143–150.
- [78] Pedragosa-Badia, X., Stichel, J., Beck-Sickinger, A.G., 2013. Neuropeptide Y receptors: how to get subtype selectivity. *Frontiers in Endocrinology* 4:5.
- [79] Khan, I.U., Zwanziger, D., Bohme, I., Javed, M., Naseer, H., Hyder, S.W., et al., 2010. Breast-cancer diagnosis by neuropeptide Y analogues: from synthesis to clinical application. *Angewandte Chemie* 49(6):1155–1158.
- [80] Langer, M., Kratz, F., Rothen-Rutishauser, B., Wunderli-Allenspach, H., Beck-Sickinger, A.G., 2001. Novel peptide conjugates for tumor-specific chemotherapy. *Journal of Medicinal Chemistry* 44(9):1341–1348.
- [81] Bard, J.A., Walker, M.W., Brancheck, T.A., Weinshank, R.L., 1995. Cloning and functional expression of a human Y4 subtype receptor for pancreatic polypeptide, neuropeptide Y, and peptide YY. *Journal of Biological Chemistry* 270(45):26762–26765.
- [82] Lundell, I., Blomqvist, A.G., Berglund, M.M., Schober, D.A., Johnson, D., Statnick, M.A., et al., 1995. Cloning of a human receptor of the NPY receptor family with high affinity for pancreatic polypeptide and peptide YY. *Journal of Biological Chemistry* 270(49):29123–29128.
- [83] Widdowson, P.S., 1993. Quantitative receptor autoradiography demonstrates a differential distribution of neuropeptide-Y Y1 and Y2 receptor subtypes in human and rat brain. *Brain Research* 631(1):27–38.
- [84] Cao, X., Zhang, L., Chen, C., Wang, Q., Guo, L., Ma, Q., et al., 2017. The critical role of ABCG1 and PPARgamma/LXRalpha signaling in TLR4 mediates inflammatory responses and lipid accumulation in vascular smooth muscle cells. *Cell and Tissue Research* 368(1):145–157.
- [85] Shen, X., Li, H., Li, W., Wu, X., Sun, Z., Ding, X., 2017. Telmisartan ameliorates adipoR1 and adipoR2 expression via PPAR-gamma activation in the coronary artery and VSMCs. *Biomedicine & Pharmacotherapy = Biomedecine & Pharmacotherapie* 95:129–136.
- [86] Modin, A., Malmstrom, R.E., Meister, B., 1999. Vascular neuropeptide Y Y1-receptors in the rat kidney: vasoconstrictor effects and expression of Y1-receptor mRNA. *Neuropeptides* 33(4):253–259.
- [87] Cheng, C.F., Chen, H.H., Lin, H., 2010. Role of PPARalpha and its agonist in renal diseases. *PPAR Research* 2010:345098.
- [88] Cabre, A., Lazaro, I., Girona, J., Manzanares, J.M., Marimon, F., Plana, N., et al., 2007. Fatty acid binding protein 4 is increased in metabolic syndrome and with thiazolidinedione treatment in diabetic patients. *Atherosclerosis* 195(1):150–158.
- [89] Furukawa, H., Mawatari, K., Koyama, K., Yasui, S., Morizumi, R., Shimohata, T., et al., 2011. Telmisartan increases localization of glucose transporter 4 to the plasma membrane and increases glucose uptake via peroxisome proliferator-activated receptor gamma in 3T3-L1 adipocytes. *European Journal of Pharmacology* 660(2–3):485–491.
- [90] Kralisch, S., Fasshauer, M., 2013. Adipocyte fatty acid binding protein: a novel adipokine involved in the pathogenesis of metabolic and vascular disease? *Diabetologia* 56(1):10–21.
- [91] Pelton, P.D., Zhou, L., Demarest, K.T., Burris, T.P., 1999. PPARgamma activation induces the expression of the adipocyte fatty acid binding protein gene in human monocytes. *Biochemical and Biophysical Research Communications* 261(2):456–458.
- [92] Yamauchi, T., Kamon, J., Waki, H., Terauchi, Y., Kubota, N., Hara, K., et al., 2001. The fat-derived hormone adiponectin reverses insulin resistance associated with both lipodystrophy and obesity. *Nature Medicine* 7(8):941–946.
- [93] Cha, D.R., Zhang, X., Zhang, Y., Wu, J., Su, D., Han, J.Y., et al., 2007. Peroxisome proliferator activated receptor alpha/gamma dual agonist tesaglitazar attenuates diabetic nephropathy in db/db mice. *Diabetes* 56(8):2036–2045.
- [94] Chira, E.C., McMillen, T.S., Wang, S., Haw 3rd, A., O'Brien, K.D., Wight, T.N., et al., 2007. Tesaglitazar, a dual peroxisome proliferator-activated receptor alpha/gamma agonist, reduces atherosclerosis in female low density lipoprotein receptor deficient mice. *Atherosclerosis* 195(1):100–109.
- [95] Coleman, D.L., 1978. Obese and diabetes: two mutant genes causing diabetes-obesity syndromes in mice. *Diabetologia* 14(3):141–148.
- [96] Zhang, Y., Proenca, R., Maffei, M., Barone, M., Leopold, L., Friedman, J.M., 1994. Positional cloning of the mouse obese gene and its human homologue. *Nature* 372(6505):425–432.
- [97] Brand, C.L., Sturis, J., Gotfredsen, C.F., Fleckner, J., Fledelius, C., Hansen, B.F., et al., 2003. Dual PPARalpha/gamma activation provides enhanced improvement of insulin sensitivity and glycemic control in ZDF rats. *American Journal of Physiology - Endocrinology And Metabolism* 284(4):E841–E854.
- [98] Coleman, D.L., Hummel, K.P., 1973. The influence of genetic background on the expression of the obese (Ob) gene in the mouse. *Diabetologia* 9(4):287–293.
- [99] Lee, S.M., Bressler, R., 1981. Prevention of diabetic nephropathy by diet control in the db/db mouse. *Diabetes* 30(2):106–111.
- [100] Harrity, T., Farrelly, D., Tieman, A., Chu, C., Kunselman, L., Gu, L., et al., 2006. Muraglitazar, a novel dual (alpha/gamma) peroxisome proliferator-activated receptor activator, improves diabetes and other metabolic abnormalities and preserves beta-cell function in db/db mice. *Diabetes* 55(1):240–248.
- [101] Arita, Y., Kihara, S., Ouchi, N., Takahashi, M., Maeda, K., Miyagawa, J., et al., 1999. Paradoxical decrease of an adipose-specific protein, adiponectin, in obesity. *Biochemical and Biophysical Research Communications* 257(1):79–83.
- [102] Floegel, A., Stefan, N., Yu, Z., Mühlenbruch, K., Drogan, D., Joost, H.G., et al., 2013. Identification of serum metabolites associated with risk of type 2 diabetes using a targeted metabolomic approach. *Diabetes* 62(2):639–648.
- [103] Giesbertz, P., Padberg, I., Rein, D., Ecker, J., Hofle, A.S., Spanier, B., et al., 2015. Metabolite profiling in plasma and tissues of ob/ob and db/db mice identifies novel markers of obesity and type 2 diabetes. *Diabetologia* 58(9):2133–2143.
- [104] O'Neill, S., Bohl, M., Gregersen, S., Hermansen, K., O'Driscoll, L., 2016. Blood-Based biomarkers for metabolic syndrome. *Trends in Endocrinology and Metabolism—TEM* 27(6):363–374.
- [105] Rohlfing, C.L., Little, R.R., Wiedmeyer, H.M., England, J.D., Madsen, R., Harris, M.J., et al., 2000. Use of GbH (HbA1c) in screening for undiagnosed diabetes in the U.S. population. *Diabetes Care* 23(2):187–191.
- [106] Xiang, L., Cheang, W.S., Lin, S.H., Wang, L., Li, Y.L., Huang, Y., et al., 2015. Plasma metabolic signatures reveal the regulatory effect of exercise training in db/db mice. *Molecular BioSystems* 11(9):2588–2596.
- [107] Xiang, L., Zhang, H., Wei, J., Tian, X.Y., Luan, H., Li, S., et al., 2018. Metabolomics studies on db/db diabetic mice in skeletal muscle reveal effective clearance of overloaded intermediates by exercise. *Analytica Chimica Acta* 1037:130–139.
- [108] Boden, G., 1997. Role of fatty acids in the pathogenesis of insulin resistance and NIDDM. *Diabetes* 46(1):3–10.

- [109] Sugii, S., Olson, P., Sears, D.D., Saberi, M., Atkins, A.R., Barish, G.D., et al., 2009. PPARgamma activation in adipocytes is sufficient for systemic insulin sensitization. *Proceedings of the National Academy of Sciences of the United States of America* 106(52):22504–22509.
- [110] Bays, H., Mandarino, L., DeFronzo, R.A., 2004. Role of the adipocyte, free fatty acids, and ectopic fat in pathogenesis of type 2 diabetes mellitus: peroxisomal proliferator-activated receptor agonists provide a rational therapeutic approach. *Journal of Clinical Endocrinology & Metabolism* 89(2): 463–478.
- [111] Ericsson, H., Hamren, B., Bergstrand, S., Elebring, M., Fryklund, L., Heijer, M., et al., 2004. Pharmacokinetics and metabolism of tesaglitazar, a novel dual-acting peroxisome proliferator-activated receptor alpha/gamma agonist, after a single oral and intravenous dose in humans. *Drug Metabolism & Disposition— The Biological Fate of Chemicals* 32(9):923–929.
- [112] Bravo-Nuevo, A., Sugimoto, H., Iyer, S., Fallon, Z., Lucas, J.M., Kazerounian, S., et al., 2011. RhoB loss prevents streptozotocin-induced diabetes and ameliorates diabetic complications in mice. *The American Journal of Pathology* 178(1):245–252.
- [113] Zhang, Y., Chen, K., Guo, L., Wu, C., 2002. Characterization of PINCH-2, a new focal adhesion protein that regulates the PINCH-1-ILK interaction, cell spreading, and migration. *The Journal of Biological Chemistry* 277(41): 38328–38338.
- [114] Bluteau, G., Zhuang, L., Amann, R., Trueb, B., 2014. Targeted disruption of the intracellular domain of receptor FgfrL1 in mice. *PLoS One* 9(8):e105210.
- [115] Kahkonen, T.E., Ivaska, K.K., Jiang, M., Buki, K.G., Vaananen, H.K., Harkonen, P.L., 2018. Role of fibroblast growth factor receptors (FGFR) and FGFR like-1 (FGFRL1) in mesenchymal stromal cell differentiation to osteoblasts and adipocytes. *Molecular and Cellular Endocrinology* 461:194–204.
- [116] Jiao, H., Arner, P., Dickson, S.L., Vidal, H., Mejhert, N., Henegar, C., et al., 2011. Genetic association and gene expression analysis identify FGFR1 as a new susceptibility gene for human obesity. *The Journal of Clinical Endocrinology and Metabolism* 96(6):E962–E966.
- [117] Fruebis, J., Tsao, T.S., Javorschi, S., Ebbets-Reed, D., Erickson, M.R., Yen, F.T., et al., 2001. Proteolytic cleavage product of 30-kDa adipocyte complement-related protein increases fatty acid oxidation in muscle and causes weight loss in mice. *Proceedings of the National Academy of Sciences of the United States of America* 98(4):2005–2010.
- [118] Mayerson, A.B., Hundal, R.S., Dufour, S., Lebon, V., Befroy, D., Cline, G.W., et al., 2002. The effects of rosiglitazone on insulin sensitivity, lipolysis, and hepatic and skeletal muscle triglyceride content in patients with type 2 diabetes. *Diabetes* 51(3):797–802.
- [119] Trayhurn, P., 1979. Thermoregulation in the diabetic-obese (db/db) mouse. The role of non-shivering thermogenesis in energy balance. *Pflugers Archiv – European Journal of Physiology* 380(3):227–232.
- [120] Pulong, W.P., Ushikai, M., Arimura, E., Abe, M., Kawaguchi, H., Horiuchi, M., 2018. Food intake and core body temperature of pups and adults in a *db* mouse line deficient in the long form of the leptin receptor without misty mutation. *Journal of diabetes research* 2018:9670871.
- [121] Bouali, S.M., Fournier, A., St-Pierre, S., Jolicoeur, F.B., 1995. Effects of NPY and NPY2-36 on body temperature and food intake following administration into hypothalamic nuclei. *Brain Research Bulletin* 36(2):131–135.
- [122] Felies, M., von Horsten, S., Pabst, R., Nave, H., 2004. Neuropeptide Y stabilizes body temperature and prevents hypotension in endotoxaemic rats. *The Journal of Physiology* 561(Pt 1):245–252.
- [123] Wallenius, K., Kjellstedt, A., Thalen, P., Lofgren, L., Oakes, N.D., 2013. The PPAR alpha / gamma agonist, tesaglitazar, improves insulin mediated switching of tissue glucose and free fatty acid utilization in vivo in the obese Zucker rat. *PPAR Research* 2013:305347.
- [124] Liao, J., Soltani, Z., Ebenezer, P., Isidro-Carrion, A.A., Zhang, R., Asghar, A., et al., 2010. Tesaglitazar, a dual peroxisome proliferator-activated receptor agonist (PPAR alpha/gamma), improves metabolic abnormalities and reduces renal injury in obese Zucker rats. *Nephron. Experimental Nephrology* 114(2): e61–e68.